



Na, J., Huang, Y., Wu, X., Gao, G., Herrmann, G., & Jiang, J. Z.
(2017). Active Adaptive Estimation and Control for Vehicle
Suspensions With Prescribed Performance. *IEEE Transactions on
Control Systems Technology*.
<https://doi.org/10.1109/TCST.2017.2746060>

Peer reviewed version

Link to published version (if available):
[10.1109/TCST.2017.2746060](https://doi.org/10.1109/TCST.2017.2746060)

[Link to publication record in Explore Bristol Research](#)
PDF-document

This is the author accepted manuscript (AAM). The final published version (version of record) is available online via IEEE at <http://ieeexplore.ieee.org/document/8053460/>. Please refer to any applicable terms of use of the publisher.

University of Bristol - Explore Bristol Research

General rights

This document is made available in accordance with publisher policies. Please cite only the published version using the reference above. Full terms of use are available:
<http://www.bristol.ac.uk/red/research-policy/pure/user-guides/ebr-terms/>

Adaptive Estimation and Control for Vehicle Active Suspensions with Prescribed Performance

Jing Na, Yingbo Huang, Xing Wu, Guanbin Gao, Guido Herrmann and Jason Zheng Jiang

Abstract—This paper proposes an adaptive control for vehicle active suspensions with unknown nonlinearities (e.g. nonlinear springs and piece-wise dampers). A prescribed performance function (PPF) that characterizes the convergence rate, maximum overshoot and steady-state error is incorporated into the control design to stabilize the vertical and pitch motions, such that both the transient and steady-state suspension response are guaranteed. Moreover, a novel adaptive law is used to achieve precise estimation of essential parameters (e.g. mass of vehicle body and moment of inertia for pitch motion), where the parameter estimation error is obtained explicitly and then used as a new leakage term. Theoretical studies prove the convergence of the estimated parameters, and compare the suggested controller with generic adaptive controllers using the gradient descent and e-modification schemes. In addition to motion displacements, dynamic tire loads and suspension travel constraints are also considered. Extensive comparative simulations on a dynamic simulator consisting of commercial vehicle simulation software Carsim[®] 8.1 and Matlab[®] Simulink are provided to show the efficacy of the proposed control, and to illustrate the improved performance.

Index Terms—Active suspension systems, adaptive control, parameter estimation, prescribed performance, neural network.

I INTRODUCTION

WITH the current growth of the automotive industry, the design of vehicle suspension systems has drawn considerable attention due to its potential to improve the ride comfort, vehicle maneuverability and safety of passengers [1, 2]. Vehicle suspension systems usually consist of wishbone, springs, and shock absorbers (e.g. dampers) to transmit and filter all forces between the car body and the road. In particular, springs are used to isolate the car body from the road disturbances and thus improve passenger comfort, while dampers are devoted to the damping of body and wheel oscillations for improved ride safety [3]. In the past decades, various suspension systems have been investigated, e.g. passive suspensions, semi-active suspensions and active suspensions [4-9]. Among these methods, active suspensions are able to add and dissipate energy from systems by using extra actuators placed between the car body and the wheel-axle [10]. Thus, active suspensions may result in higher energy demand in comparison to semi-active suspension,

which should be managed in the control design. However, active suspensions can achieve better performance than passive and semi-active suspensions. Thus, considerable work has recently been carried out [11-14] on the development of active suspension controllers in vehicle systems.

In active suspension systems, actuators are used to provide extra control actions to shape the suspension motions; thus, the limitation from such motions and the firm uninterrupted contact of the wheels to the road must be ensured. In this respect, the requirements for active vehicle suspensions may include motion displacements, dynamic tire loads and suspension travel constraints, etc., and the trade-off between these conflicting requirements should be carefully addressed in the control synthesis. To this end, an adaptive control was proposed in [15] to achieve multi-degree-of-freedom (DOF) isolation of a skyhook target. In [16], a robust control was designed based on a quarter-car model. An H_∞ control [17] was used for active suspension systems. A Linear Quadratic Gaussian (LQG) control was also considered in [18]. **Although these optimal control or robust control schemes can address the control constraints, the system dynamics studied in aforementioned results are assumed to be linear.**

However, in practical vehicle systems, uncertainties and/or nonlinearities are unavoidable. To address these parameter uncertainties and unknown nonlinearities, e.g. nonlinear springs, piece-wise dampers and the change of the vehicle weights, a sliding mode control has been used in [19, 20]. Specifically, a neural network (NN) was incorporated into backstepping control in [20]. However, only parts of the suspension performance, e.g. the oscillation amplitude of the sprung mass, were studied. To study other suspension requirements, an adaptive backstepping control was given in [21], where the dynamic tire loads, suspension travel and actuator saturations are all considered. Nevertheless, the nonlinear stiffening spring and damper dynamics are assumed to be known, and only the vehicle mass and the mass moment of inertia for the pitch motion are online updated in [21]. Moreover, according to the certainty equivalence principle [22], if the estimated parameters in adaptive control converge to their actual values, the performance of the overall control system can be greatly improved. Thus, it is also desirable to investigate new adaptive laws that are able to guarantee the convergence of the estimated parameters to their true values.

On the other hand, most available active suspension control designs, e.g. [8, 9, 21], can prove steady-state suspension convergence, however, their transient suspension response (e.g. maximum overshoot and convergence rate) cannot be prescribed through control design. From the perspective of safe operation and ride comfort, it is preferable to guarantee

Manuscript received XXX, 2016; revised XXX 2016; accepted XXX. Date of publication XXX; date of current version XXX. This work was supported by National Natural Science Foundation of China under Grant 61573174, and in part by the Marie Curie Intra-European Fellowships AECE Project under Grant FP7-PEOPLE-2013-IEF-625531.

Jing Na, Yingbo Huang, Xing Wu and Guanbin Gao are with the Faculty of Mechanical & Electrical Engineering, Kunming University of Science & Technology, Kunming, 650500, P.R. China (E-mail: najing25@163.com). Guido Herrmann and Jason Zheng Jiang are with the Department of Mechanical Engineering, University of Bristol, BS8 1TR, UK.

both the transient and steady-state suspension response.

Motivated by these observations, this paper presents an alternative adaptive control for active vehicle suspension systems with unknown nonlinear spring and piece-wise damper dynamics. One salient feature of the proposed control is that both the transient and steady-state suspension response can be strictly guaranteed. This is achieved by incorporating a prescribed performance function (PPF) [23-26] into adaptive control. An augmented NN is then used to compensate for the unknown dynamics. Another advantage of the studied control lies in that the parameters (e.g. mass of vehicle body, inertia for pitch motion) are online updated. These estimated parameters converge to their true values by using a newly developed adaptive law [27], where a new leakage term of the parameter estimation error [28] is superimposed on the classical adaptation method. The suspension performance requirements, e.g. the vertical and pitch motion displacements, dynamic tire loads and suspension travel constraints, are also studied. A rigorous theoretical analysis is the basis for comparisons with several other adaptive laws (e.g. gradient, *e*-modification). The actuator dynamics and the actuator saturation problem are also considered by including electrical linear motors and an anti-windup compensator. Finally, simulations with a half-car system built in a combined simulator with Carsim[®] 8.1 and Matlab[®] Simulink are carried out to illustrate the efficacy of the proposed methods.

The paper is organized as follows: The problem formulation is given in Section II. Section III proposes an adaptive control design with a new adaptive law and a relevant stability analysis. Section IV compares the proposed method with other adaptive controllers. Section V considers the actuator dynamics and the saturation compensation. Simulations are provided in Section VI. Conclusions are given in Section VII.

II PROBLEM FORMULATION

In this paper, a nonlinear half-car suspension system is studied. As shown in Fig.1, M and I are the unknown mass of the vehicle body and the mass moment of inertia for the pitch motion; m_f and m_r are the unsprung masses of front and rear wheels; F_{df}, F_{dr}, F_{sf} and F_{sr} are the forces produced by the dampers and springs; F_{yf}, F_{bf}, F_{tr} and F_{br} denote the elasticity forces and damping forces of the tires. For the vehicle body, y_c is the vertical displacement and φ is the pitch angle, y_1, y_2 are the displacements of the unsprung mass, y_{o1}, y_{o2} are the road inputs to the wheels. a, b define the distances between the suspension system to the vehicle body center, and u_1, u_2 are the actuator inputs.

The nonlinear dynamics of the studied suspension system in Fig.1 can be obtained based on Newton's law as [21]:

$$\begin{cases} M\ddot{y}_c + F_{df} + F_{dr} + F_{sf} + F_{sr} = u_y + d_1 \\ I\ddot{\varphi} + a(F_{df} + F_{sf}) - b(F_{dr} + F_{sr}) = u_\varphi + d_2 \\ m_f\ddot{y}_1 - F_{sf} - F_{dr} + F_{yf} + F_{bf} = -u_1 + d_3 \\ m_r\ddot{y}_2 - F_{sr} - F_{dr} + F_{tr} + F_{br} = -u_2 + d_4 \end{cases} \quad (1)$$

where $u_y = u_1 + u_2$ and $u_\varphi = au_1 - bu_2$ are the control actions

used to determine the actual control signals u_1, u_2 . The bounded terms $d_i, i=1,2,3,4$ denote the **lumped effect** of sensor noise, external disturbances and modeling uncertainties. Note that in practical applications, actuators should be used to create the control actions u_1, u_2 , and their dynamics will be considered in Section V.

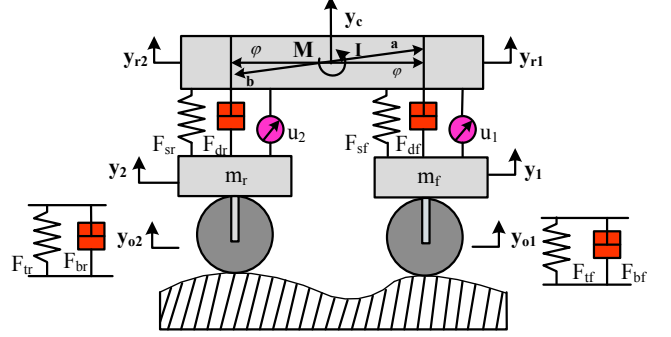


Fig.1. Schematic of half-car model with active suspension.

In practice, the active suspension control design should consider the driving comfort, safety and hardware limitations, etc. Without loss of generality, the following widely used performance requirements (e.g. [21]) are considered:

1) *Motion displacements*. The vertical displacement y_c and pitch motion angle φ can be attenuated via the control signals u_1, u_2 , so that the vehicle body can be isolated as far as possible from the road-induced shocks.

2) *Dynamic tire loads*. In order to assure driving safety, the firm uninterrupted contact of the wheels to the road must be ensured, i.e. the dynamic tire loads should not be too large for both the front and rear wheels, that is,

$$|Z_f| = |F_{yf} + F_{bf}| < F_f, |Z_r| = |F_{tr} + F_{br}| < F_r \quad (2)$$

where the allowable tire loads F_f and F_r are calculated by

$$\begin{aligned} F_f + F_r &= (M + m_f + m_r)g \\ F_f(a + b) &= Mgb + m_f g(a + b) \end{aligned} \quad (3)$$

3) *Suspension travel constraints*. Due to the limited mechanical space, the suspension travel defined by [21]

$$\Delta y_f = y_c + a \sin \varphi - y_1, \Delta y_r = y_c - b \sin \varphi - y_2 \quad (4)$$

must be limited by the maximum suspension deflections $\Delta y_{f \max}$ and $\Delta y_{r \max}$ as

$$|\Delta y_f| < \Delta y_{f \max}, |\Delta y_r| < \Delta y_{r \max}. \quad (5)$$

Remark 1: System (1) has been widely used to represent essential characteristics of the vertical and pitch motions. Some adaptive controllers have been proposed to regulate the vertical displacement for (1), e.g. [21] and references therein. However, in standard adaptive control, the transient response (e.g. overshoot and convergence rate) of the car body motions y_c and φ cannot be prescribed. Moreover, there are some unknown parameters (e.g. M and I), which need to be specified to fulfill the conditions (2)-(5).

In this paper, we will propose an alternative control scheme by introducing prescribed performance functions [24, 25] and using recently proposed adaptive laws [27], such that the transient and steady-state suspension responses of y_c

and φ can be designed *a priori*. Moreover, the convergence of the estimated parameters to their true values M and I are to be achieved. It should be noted that the spring and piecewise damper dynamics F_{df}, F_{dr}, F_{sf} and F_{sr} are nonlinear and unknown in this paper, which will be compensated online with neural networks (NNs).

To facilitate the control design, we define the system state variables as

$$\begin{aligned} x_1 &= y_c, x_2 = \dot{y}_c, x_3 = \varphi, x_4 = \dot{\varphi}, \\ x_5 &= y_1, x_6 = \dot{y}_1, x_7 = y_2, x_8 = \dot{y}_2 \end{aligned} \quad (6)$$

Then system (1) is rewritten in a state-space form:

$$\begin{cases} \dot{x}_1 = x_2 \\ \dot{x}_2 = \theta_1(-F_{df} - F_{dr} - F_{sf} - F_{sr} + u_y + d_1) \\ \dot{x}_3 = x_4 \\ \dot{x}_4 = \theta_2[-a(F_{df} + F_{sf}) + b(F_{dr} + F_{sr}) + u_\varphi + d_2] \end{cases} \quad (7)$$

$$\begin{cases} \dot{x}_5 = x_6 \\ \dot{x}_6 = \frac{1}{m_f}(F_{sf} + F_{df} - F_{yf} - F_{bf} - u_1 + d_3) \\ \dot{x}_7 = x_8 \\ \dot{x}_8 = \frac{1}{m_r}(F_{sr} + F_{dr} - F_{tr} - F_{br} - u_2 + d_4) \end{cases} \quad (8)$$

where $\theta_1 = 1/M$ and $\theta_2 = 1/I$ are the unknown parameters.

It is noted that θ_1 and θ_2 will vary with the changes of the vehicle weights (e.g. number of passengers and/or payloads). Thus, precise online estimation of θ_1 , θ_2 is essential in the control design for the safe operation of vehicles.

III ADAPTIVE CONTROL WITH GUARANTEED PERFORMANCE

In this section, an adaptive control is proposed for (7)-(8) to regulate the vertical and pitch motions. The control of vertical displacement x_1 is studied at first, and the control of pitch motion x_3 can be obtained similarly. Other suspension requirements (2) and (5) are also analyzed.

A. Adaptive PPF Control for Vertical Displacement

To guarantee a prescribed control bound of x_1 , a positive decreasing function $\varphi_i(t): R^+ \rightarrow R^+$ will be used as the prescribed performance function [23, 29]

$$\varphi_i(t) = (\varphi_{i0} - \varphi_{i\infty})e^{-\alpha_i t} + \varphi_{i\infty}, i = 1, 2 \quad (9)$$

where $\varphi_{i0} > \varphi_{i\infty}$ and $\alpha_i > 0$ are the design parameters, and thus $\lim_{t \rightarrow \infty} \varphi_i(t) = \varphi_{i\infty} > 0$ is true. Note that $i = 1, 2$ refers to the vertical and pitch dynamics in this paper, respectively.

The objective is to retain x_1 within the bound

$$-\underline{\delta}\varphi_1(t) < x_1(t) < \bar{\delta}\varphi_1(t), \forall t > 0 \quad (10)$$

where $\underline{\delta}, \bar{\delta}$ are positive constants chosen by the designers. Clearly, the transient and steady-state regulation performance of x_1 can be determined by (10). In particular, $-\underline{\delta}\varphi_1(0)$ and $\bar{\delta}\varphi_1(0)$ represent the lower bound of an undershoot and the upper bound of an overshoot. The scalar α_i defines the

convergence rate and $\varphi_{i\infty}$ denotes the allowable steady-state error [24, 25]. Thus, both the transient and steady-state performance can be designed *a priori* by appropriately tuning the parameters $\underline{\delta}, \bar{\delta}, \alpha_i, \varphi_{i0}$ and $\varphi_{i\infty}$.

We will design u_y such that (10) can be guaranteed for all time. The basic idea of the following developments is to transform the control problem of (7) with constraint (10) into an equivalent ‘unconstrained’ control problem as [23-26, 30]. For this purpose, we define a smooth and strictly increasing function $S(z_1)$ of the transformed signal $z_1 \in R$, such that

$$\begin{aligned} 1) \quad & -\underline{\delta} < S(z_1) < \bar{\delta}, \forall z_1 \in L_\infty \\ 2) \quad & \lim_{z_1 \rightarrow +\infty} S(z_1) = \bar{\delta}, \lim_{z_1 \rightarrow -\infty} S(z_1) = -\underline{\delta} \end{aligned}$$

Then according to the properties of $S(z_1)$, x_1 can be represented to enforce condition (10) as:

$$x_1 = \varphi_1(t)S(z_1). \quad (11)$$

Considering the fact that $S(z_1)$ is strictly monotonically increasing and $\varphi_{10}(t) \geq \varphi_{1\infty} > 0$, the inverse function of $S(z_1)$ exists such that:

$$z_1 = S^{-1}\left[\frac{x_1}{\varphi_1}\right]. \quad (12)$$

For any initial condition $x_1(0)$, if the parameters $\bar{\delta}, \underline{\delta}$ and φ_{10} are chosen such that $-\underline{\delta}\varphi_1(0) < x_1(0) < \bar{\delta}\varphi_1(0)$, and z_1 can be controlled to be bounded (i.e. $z_1 \in L_\infty, \forall t > 0$) via u_y , one may verify that $-\underline{\delta} < S(z_1) < \bar{\delta}$ holds, and $-\underline{\delta}\varphi_1(t) < x_1(t) < \bar{\delta}\varphi_1(t)$ can be retained. Hence, the control of system (7) with constraint (10) can be achieved by stabilizing the coordinate z_1 in (12). We have:

Lemma 1 [23]: System (7) is invariant under the transform (12) with $S(z_1)$, thus the stabilization of the coordinate z_1 can guarantee the regulation of x_1 with constraint (10).

In this paper, we choose the function $S(z_1)$ as in [25]:

$$S(z_1) = \frac{\bar{\delta}e^{z_1} - \underline{\delta}e^{-z_1}}{e^{z_1} + e^{-z_1}}. \quad (13)$$

Then the transformed error z_1 can be obtained as:

$$z_1 = S^{-1}\left[\frac{x_1(t)}{\varphi_1(t)}\right] = \frac{1}{2} \ln \frac{\mu_1(t) + \underline{\delta}}{\bar{\delta} - \mu_1(t)} \quad (14)$$

where $\mu_1(t) = x_1(t)/\varphi_1(t)$ is a measurable variable. Hence, one can calculate the derivatives of z_1 as:

$$\begin{aligned} \dot{z}_1 &= \frac{\partial S^{-1}}{\partial \mu_1} \dot{\mu}_1 = \frac{1}{2} \left[\frac{1}{\mu_1 + \underline{\delta}} - \frac{1}{\mu_1 - \bar{\delta}} \right] \left(\frac{\dot{x}_1}{\varphi_1} - \frac{x_1 \dot{\varphi}_1}{\varphi_1^2} \right) \\ &= \tau_1 \left(x_2 - \frac{x_1 \dot{\varphi}_1}{\varphi_1} \right) \end{aligned} \quad (15)$$

and

$$\begin{aligned} \ddot{z}_1 &= \dot{\tau}_1 \left(x_2 - \frac{x_1 \dot{\varphi}_1}{\varphi_1} \right) - \tau_1 \left(\frac{x_2 \dot{\varphi}_1}{\varphi_1} + \frac{x_1 \ddot{\varphi}_1}{\varphi_1} - \frac{x_1 \dot{\varphi}_1^2}{\varphi_1^2} \right) \\ &\quad + \tau_1 \theta_1 (-F_{df} - F_{dr} - F_{sf} - F_{sr} + u_y + d_1) \end{aligned} \quad (16)$$

where $\tau_1 = (1/2\varphi_1)[1/(\mu_1 + \underline{\delta}) - 1/(\mu_1 - \bar{\delta})]$ is calculated based

on x_1 and φ_1 , which is positive and bounded.

According to Lemma 1, the PPF bound (10) can be guaranteed if z_1 can be controlled to be bounded by u_y . To achieve this purpose, we define the filtered error as:

$$s_{p1} = [\Lambda_{p1}, 1][z_1, \dot{z}_1]^T \quad (17)$$

where $\Lambda_{p1} > 0$ is a positive constant such that the error z_1 is bounded as long as s_{p1} is bounded [22].

Furthermore, we can obtain the time derivative of s_{p1} as

$$\dot{s}_{p1} = T_{p1}(Z_{p1}) + \tau_1 \theta_1 u_y + \tau_1 \theta_1 d_1 \quad (18)$$

where $Z_{p1} = [x_1, x_2]$ and $T_{p1}(Z_{p1}) = (\Lambda_{p1} \tau_1 + \dot{\tau}_1)(x_2 - \frac{x_1 \dot{\varphi}_1}{\varphi_1})$

$-\tau_1(\frac{x_2 \dot{\varphi}_1}{\varphi_1} + \frac{x_1 \ddot{\varphi}_1}{\varphi_1} - \frac{x_1 \dot{\varphi}_1^2}{\varphi_1^2}) + \tau_1 \theta_1 (-F_{df} - F_{dr} - F_{sf} - F_{sr})$ is a lumped (unknown) term of the damper and spring dynamics. It can be approximated by a NN [31-35] as

$$T_{p1}(Z_{p1}) = w_{p1}^T \phi_{p1}(Z_{p1}) + \varepsilon_{p1}, \forall Z_{p1} \in R^{L_p} \quad (19)$$

where $w_{p1} = [w_{p11}, w_{p12}, \dots, w_{p1L_p}]^T \in R^{L_p}$ is the NN weight and $\varepsilon_{p1} \in R$ is the approximation error. They are bounded by $\|w_{p1}\| \leq w_{p1N}$, $|\varepsilon_{p1}| < \varepsilon_{p1N}$ for positive constants w_{p1N} and ε_{p1N} , $\phi_{p1}(Z_{p1}) = [\phi_{p11}, \phi_{p12}, \dots, \phi_{p1L_p}]^T$ is the regressor vector. The notation of $T_{p1}(Z_{p1})$ shows that it is a function of the vertical displacement x_1 and velocity x_2 . In this case, some commercial sensors (e.g. accelerometer or laser sensor [14, 36]) can be used to provide the required measurements for the NN and feedback control. Sensor noise can be taken as a part of the disturbance d_1 .

In this case, \dot{s}_{p1} in (18) can be written as

$$\dot{s}_{p1} = w_{p1}^T \phi_{p1}(Z_{p1}) + \varepsilon_{p1} + \tau_1 \theta_1 u_y. \quad (20)$$

where $\varepsilon_{p1} = \varepsilon_{p1n} + \tau_1 \theta_1 d_1$ denotes the lumped residual error defining the effect of bounded NN-error and disturbance, and thus $|\varepsilon_{p1}| < \varepsilon_{p1N}$ holds for a positive constant ε_{p1N} .

Now, we design the following control u_y to stabilize (20)

$$u_y = \frac{1}{\tau_1 \hat{\theta}_1} [-k_{p1} s_{p1} - \hat{w}_{p1}^T \phi_{p1}(Z_{p1})] \quad (21)$$

where $k_{p1} > 0$ is a positive feedback control gain, $\hat{\theta}_1$ is the estimation of the uncertain parameter θ_1 , and \hat{w}_{p1} is the estimation of the NN weight w_{p1} , which will be updated via the adaptive law (26).

Remark 2: In classical adaptive control for (20)-(21), e.g. [22], the gradient descent adaptation or modified version with projection [21] was used to estimate the NN weight w_{p1} and the parameter θ_1 by minimizing the control error s_{p1} . However, in these algorithms the convergence of the estimates to their true values may be difficult due to the modeling errors and the induced damping effect in the adaptive laws. This will be analyzed in Section IV.

Different to classical adaptive laws, we will propose a novel adaptive law as in [27] to guarantee the convergence of

the parameter estimation and control error simultaneously. Thus, (20) can be written as

$$\dot{s}_{p1} = w_{p1}^T \phi_{p1}(Z_{p1}) + \varepsilon_{p1} + \tau_1 \theta_1 u_y = W_{p1}^T \Phi_{p1} + \varepsilon_{p1} \quad (22)$$

where $W_{p1} = [w_{p1}^T, \theta_1]^T$ and $\Phi_{p1} = [\phi_{p1}^T(Z_{p1}), \tau_1 u_y]^T$ are the augmented parameter and the regressor vector, respectively.

Then, we define the filtered variables s_{p1f}, Φ_{p1f} as

$$\begin{cases} k \dot{s}_{p1f} + s_{p1f} = s_{p1}, & s_{p1f}(0) = 0 \\ k \dot{\Phi}_{p1f} + \Phi_{p1f} = \Phi_{p1}, & \Phi_{p1f}(0) = 0 \end{cases} \quad (23)$$

and the auxiliary matrix P_{p1} and vector Q_{p1} as

$$\begin{cases} \dot{P}_{p1} = -l P_{p1} + \Phi_{p1f} \Phi_{p1f}^T, & P_{p1}(0) = 0 \\ \dot{Q}_{p1} = -l Q_{p1} + \Phi_{p1f} [(s_{p1} - s_{p1f})/k], & Q_{p1}(0) = 0 \end{cases} \quad (24)$$

where $k > 0$ and $l > 0$ are positive constants.

We denote an auxiliary vector H_{p1} based on P_{p1}, Q_{p1} as

$$H_{p1} = P_{p1} \hat{W}_{p1} - Q_{p1} \quad (25)$$

where \hat{W}_{p1} is the estimated vector. It is updated by the following adaptive law

$$\dot{\hat{W}}_{p1} = \Gamma_{p1} s_{p1} \Phi_{p1} - \Gamma_{p1} \sigma H_{p1} \quad (26)$$

where $\Gamma_{p1} > 0$ is the adaptive gain and $\sigma > 0$ is a constant.

In (26), a new leakage term H_{p1} is introduced, which is different to the e -modification and σ -modification [22]. To analyze the convergence of (26), we first present a lemma to show the merit of H_{p1} .

Lemma 2: Consider P_{p1}, Q_{p1} and H_{p1} defined in (24)-(25), then H_{p1} can be represented as $H_{p1} = -P_{p1} \tilde{W}_{p1} + \Delta_{p1}$, where

$$\Delta_{p1} = -\int_0^t e^{-l(t-r)} \Phi_{p1f}(r) \varepsilon_{p1f}(r) dr$$

is bounded by $\|\Delta_{p1}\| < \varepsilon_{p1Nf}$, with $k \dot{\varepsilon}_{p1f} + \varepsilon_{p1f} = \varepsilon_{p1}$; $\tilde{W}_{p1} = W_{p1} - \hat{W}_{p1}$ is the estimation error.

Proof: Please refer to Appendix-I for proof.

As shown in Lemma 2, the leakage term H_{p1} contains the information of the unknown estimation error \tilde{W}_{p1} , and thus can be used to drive the adaptive law (26) to improve the convergence of parameter estimation.

Lemma 3 [27]: If the regressor vector Φ_{p1} defined in (22) is persistently excited (PE), then the matrix P_{p1} defined in (24) is positive definite, i.e. its minimum eigenvalue fulfills $\lambda_{\min}(P_{p1}) > \sigma_{p1} > 0$ for a positive constant σ_{p1} .

Proof: We refer to [27] for a similar proof. \square

Now the main results of this section can be summarized as:

Theorem 1: Consider the vertical displacement x_1 in system (7) and the PPF control (21) with adaptive law (26). If the initial condition fulfills $-\delta \varphi_1(0) < x_1(0) < \bar{\delta} \varphi_1(0)$, and the regressor Φ_{p1} in (22) is PE, then

- 1) For the residual error $\varepsilon_{p1} = 0$, the control error s_{p1} and estimation error \tilde{W}_{p1} exponentially converge to zero;
- 2) For the residual error $\varepsilon_{p1} \neq 0$, the control error s_{p1} and estimation error \tilde{W}_{p1} converge to a small compact set.

In both cases, the vertical displacement x_1 can be retained

within the prescribed bound (10).

Proof: We refer to Appendix-II for a detailed proof. \square

Remark 3: Lemma 3 indicates that the required excitation condition $\lambda_{\min}(P_{p1}) > \sigma_{p1} > 0$ can be fulfilled under the standard PE condition, which is needed to prove the parameter estimation convergence [22]. In this sense, Lemma 3 provides an intuitive way to online verify the PE condition, i.e. one can calculate the minimum eigenvalue of matrix P_{p1} and test for $\lambda_{\min}(P_{p1}) > 0$. The proof of Lemma 3 is similar to that in [27], which we do not repeat here. It is noted that this excitation condition can usually be satisfied in vehicle suspensions due to the continuously injected disturbances y_{o1} and y_{o2} from an uneven road. Note that our algorithm augments to the gradient descent approach and it has to the least perform the same in fact better. It shows more robust convergence behavior as we present in theory and practice (see also [37]).

Remark 4: In the adaptive law (26), the first gradient term $s_{p1}\Phi_{p1}$ is used to ensure the boundedness of tracking error s_{p1} ; the new leakage term σH_{p1} contains the information of the estimation error \tilde{W}_{p1} as shown in Lemma 1. The inclusion of this leakage term in the adaptive law (26) leads to a quadratic term of \tilde{W}_{p1} in the temporal derivative of the Lyapunov function such that faster (exponential) convergence of both the control error and estimation error is obtained. In this sense, the adaptive law (26) is different to the σ -modification and e -modification superimposed on the gradient method [22], where the estimation error convergence cannot be guaranteed due to the induced damping terms. Detailed comparisons will be provided in Section IV.

B. Adaptive PPF Control for Pitch Motion

Adaptive PPF control of the pitch motion x_3 in (7) can be designed following similar manipulations as in Section III A, which can be briefly given as

$$\begin{aligned} z_2 &= S^{-1} \begin{bmatrix} x_3(t) \\ \varphi_2(t) \end{bmatrix} = \frac{1}{2} \ln \frac{\mu_2(t) + \underline{\delta}}{\bar{\delta} - \mu_2(t)}, \quad \dot{z}_2 = \tau_2 \left(x_4 - \frac{x_3 \dot{\varphi}_2}{\varphi_2} \right) \\ s_{p2} &= [\Lambda_{p2}, 1] \begin{bmatrix} z_2 \\ \dot{z}_2 \end{bmatrix}, \quad \dot{s}_{p2} = T_{p2}(Z_{p2}) + \tau_2 \theta_2 u_\varphi + \tau_2 \theta_2 d_2 \quad (27) \\ u_\varphi &= \frac{1}{\tau_2 \hat{\theta}_2} [-k_{p2} s_{p2} - \hat{w}_{p2}^T \phi_{p2}(Z_{p2})] \\ \hat{W}_{p2} &= \Gamma_{p2} s_{p2} \Phi_{p2} - \Gamma_{p2} \sigma H_{p2} \\ \text{where } \varphi_2(t) &\text{ is the PPF in (9), } \mu_2(t) = x_3(t) / \varphi_2(t), \\ \tau_2 &= (1/2\varphi_2) [1/(\mu_2 + \underline{\delta}) - 1/(\mu_2 - \bar{\delta})]; \Lambda_{p2} > 0 \text{ and } k_{p2} > 0 \\ &\text{are positive constants, } \Gamma_{p2} > 0 \text{ and } \sigma > 0 \text{ are the adaptive} \\ &\text{gains; and } T_{p2}(Z_{p2}) = (\Lambda_{p2} \tau_2 + \dot{\tau}_2) (x_4 - \frac{x_3 \dot{\varphi}_2}{\varphi_2}) - \tau_2 \left(\frac{x_4 \dot{\varphi}_2}{\varphi_2} + \frac{x_3 \ddot{\varphi}_2}{\varphi_2} - \frac{x_3 \dot{\varphi}_2^2}{\varphi_2^2} \right) \\ &+ \tau_2 \theta_2 (-a(F_{df} + F_{sf}) + b(F_{dr} + F_{sr})) = w_{p2}^T \phi_{p2}(Z_{p2}) + \varepsilon_2 \text{ are the} \\ &\text{unknown nonlinearities approximated by an NN, } \Phi_{p2} = [\phi_{p2}^T(Z_{p2}), \tau_2 u_\varphi]^T \text{ is the augmented regressor, and} \\ \hat{W}_{p2} &= [\hat{w}_{p2}^T, \hat{\theta}_2]^T \text{ is the estimate of the augmented parameter} \end{aligned}$$

$W_{p2} = [w_{p2}^T, \theta_2]^T$, $\varepsilon_{p2} = \varepsilon_2 + \tau_2 \theta_2 d_2$ is the residual error. The new leakage term H_{p2} is defined as $H_{p2} = P_{p2} \hat{W}_{p2} - Q_{p2}$ in terms of the filtered variables P_{p2}, Q_{p2} , which can be obtained similar to their counterparts P_{p1}, Q_{p1} and H_{p1} as (23)-(25). Finally, it should be noted that $T_{p2}(Z_{p2})$ is a function of the pitch displacement x_3 and velocity x_4 , which can be measured using commercial transducers [14, 36]. Hence, similar to Theorem 1, the convergence of pitch motion control (27) can be proved, which is not repeated again.

After obtaining u_y and u_φ in (21) and (27), the actual control inputs of u_1 and u_2 can be calculated as

$$u_1 = \frac{bu_y + u_\varphi}{a+b}, u_2 = \frac{au_y - u_\varphi}{a+b}. \quad (28)$$

C. Analysis of Dynamic Tire Loads and Suspension Travels

In the above analysis, the guarantee for x_1 and x_3 to remain within the prescribed bounds $-\underline{\delta}\varphi_1(t) < x_1(t) < \bar{\delta}\varphi_1(t)$ and $-\underline{\delta}\varphi_2(t) < x_3(t) < \bar{\delta}\varphi_2(t)$ has been obtained, i.e. the primary control objective 1) is achieved. In what follows, we will show that the other two suspension requirements (2) and (5) can be fulfilled by appropriately choosing parameters.

For ease of analysis, the tire forces $F_{yf}, F_{yr}, F_{bf}, F_{br}$ are modeled as in [21] as: $F_{yf} = k_{f2}(y_1 - y_{o1})$, $F_{yr} = k_{r2}(y_2 - y_{o2})$, $F_{bf} = b_{f2}(\dot{y}_1 - \dot{y}_{o1})$, $F_{br} = b_{r2}(\dot{y}_2 - \dot{y}_{o2})$, where k_{f2}, k_{r2}, b_{f2} and b_{r2} are the stiffness and damping coefficients of the tires.

We first analyze the boundedness of the state variables x_5, x_6, x_7, x_8 of (8). As indicated in Theorem 1, the vertical motions x_1, x_2 and pitch motions x_3, x_4 are bounded. Then after substitution of (28) into (8), one can obtain:

$$\dot{X} = AX + BY_0 + \omega \quad (29)$$

$$X = \begin{bmatrix} x_5 \\ x_6 \\ x_7 \\ x_8 \end{bmatrix}, Y_0 = \begin{bmatrix} y_{o1} \\ \dot{y}_{o1} \\ y_{o2} \\ \dot{y}_{o2} \end{bmatrix}, A = \begin{bmatrix} 0 & 1 & 0 & 0 \\ \frac{k_{f2}}{m_f} & -\frac{b_{f2}}{m_f} & 0 & 0 \\ 0 & 0 & 0 & 1 \\ 0 & 0 & -\frac{k_{r2}}{m_r} & -\frac{b_{r2}}{m_r} \end{bmatrix} \quad (30)$$

$$B = \begin{bmatrix} 0 & 0 & 0 & 0 \\ \frac{k_{f2}}{m_f} & \frac{b_{f2}}{m_f} & 0 & 0 \\ 0 & 0 & 0 & 0 \\ 0 & 0 & \frac{k_{r2}}{m_r} & \frac{b_{r2}}{m_r} \end{bmatrix} \quad (31)$$

$$\omega = \begin{bmatrix} 0 \\ \frac{1}{m_f(a+b)} \left(-\frac{a}{b\tau_2} \varpi_1 + \frac{ad_2}{b} + a\delta + \frac{b}{\tau_1} \varpi_2 + \frac{1}{\tau_2} \varpi_3 \right) + \frac{d_3}{m_f} \\ 0 \\ \frac{1}{m_r(a+b)} \left(-\frac{a}{b\tau_2} \varpi_1 + \frac{ad_2}{b} + b\delta + \frac{a}{\tau_1} \varpi_2 - \frac{1}{\tau_2} \varpi_3 \right) + \frac{d_4}{m_r} \end{bmatrix} \quad (32)$$

where $\delta = -\frac{w_{p1}^T \phi_{p1}(Z_{p1})}{\tau_1 \theta_1} - \frac{\varepsilon_{p1}}{\tau_1 \theta_1} + \frac{\mathcal{Q}_1}{\tau_1 \theta_1} + d_1$, $\mathcal{Q}_1 = (\Lambda_{p1} \tau_1 + \dot{\tau}_1)(x_2 - \frac{x_1 \dot{\varphi}_1}{\varphi_1})$

$$\begin{aligned}
& -\tau_1 \left(\frac{x_2 \dot{\phi}_1}{\phi_1} + \frac{x_1 \ddot{\phi}_1}{\phi_1} - \frac{x_1 \dot{\phi}_1^2}{\phi_1^2} \right), \quad \varpi_1 = -\frac{w_{p2}^T \phi_{p2}(Z_{p2})}{\theta_2} - \frac{\varepsilon_{p2}}{\theta_2} + \frac{\mathcal{G}_2}{\theta_2}, \\
& \mathcal{G}_2 = (\Lambda_{p2} \tau_2 + \dot{\tau}_2)(x_4 - \frac{x_3 \dot{\phi}_2}{\phi_2}) - \tau_2 \left(\frac{x_4 \dot{\phi}_2}{\phi_2} + \frac{x_3 \ddot{\phi}_2}{\phi_2} - \frac{x_3 \dot{\phi}_2^2}{\phi_2^2} \right), \\
& \varpi_2 = k_{p1} s_{p1} / \hat{\theta}_1 + \hat{w}_{p1}^T \phi_{p1} / \hat{\theta}_1 \quad \text{and} \quad \varpi_3 = k_{p2} s_{p2} / \hat{\theta}_2 + \hat{w}_{p2}^T \phi_{p2} / \hat{\theta}_2. \quad \text{Thus,} \\
& \omega \text{ denotes the effect of all residual errors, which is bounded because } x_1, x_2, x_3, x_4, s_{p1}, s_{p2}, \hat{w}_{p1}, \hat{w}_{p2}, \hat{\theta}_1, \hat{\theta}_2 \text{ and } d_1 \cdots d_4 \text{ are} \\
& \text{all bounded. Therefore, } \omega \text{ is bounded, i.e. } \|\omega\| \leq \varpi \text{ for a} \\
& \text{positive constant } \varpi > 0.
\end{aligned}$$

The matrix A defined in (30) is stable, i.e. there exist positive matrices $P > 0, Q > 0$ so that the Lyapunov equation $A^T P + AP = -Q$ holds. We select a Lyapunov function as $V = X^T P X$, then its derivative can be obtained along (29) as

$$\begin{aligned}
\dot{V} &= X^T (A^T P + AP) X + 2X^T P B Y_o + 2X^T P \omega \\
&\leq -[\lambda_{\min}(Q) - \frac{1}{\eta_1} \lambda_{\max}(P B B^T P) - \frac{1}{\eta_2} \lambda_{\max}(P)] \|X\|^2 \\
&\quad + \eta_1 Y_o^T Y_o + \eta_2 \lambda_{\max}(P) \varpi^2
\end{aligned} \quad (33)$$

where $\eta_1, \eta_2 > 0$ are the design parameters coming from the Young's inequality $ab \leq a^2 \eta_i / 2 + b^2 / 2 \eta_i$, $\eta_i > 0$ applied to the terms $2X^T P B Y_o, 2X^T P \omega$.

For appropriate parameters, e.g. $\eta_1 > 2\lambda_{\max}(P B B^T P) / \lambda_{\min}(Q)$, $\eta_2 > 2\lambda_{\max}(P) / \lambda_{\min}(Q)$, it follows from (33) that $\dot{V} \leq -\alpha_1 V + \beta_1$ holds, where $\alpha_1 = [\lambda_{\min}(Q) - \lambda_{\max}(P B B^T P) / \eta_1 - \lambda_{\max}(P) / \eta_2] / \lambda_{\min}(P)$ and $\beta_1 = \eta_1 \lambda_{\max}(P) y_{o \max} + \eta_2 \lambda_{\max}(P) \varpi^2$ with $Y_o^T Y_o \leq y_{o \max}$ being the road inputs. Then, we have $V(t) \leq V(0)e^{-\alpha_1 t} + \beta_1 / \alpha_1$, which implies that the variables $x_i, i = 5, 6, 7, 8$ of (8) are bounded

$$|x_i(t)| \leq \sqrt{(V(0) + \beta_1 / \alpha_1) / \lambda_{\min}(P)}, i = 5, 6, 7, 8. \quad (34)$$

Now we can address the dynamic tire load condition (2). The transferred displacements from the road disturbances to the tire deflection can be calculated as

$$\begin{aligned}
|Z_f| &\leq (k_{f2} + b_{f2}) \sqrt{(V(0) + \beta_1 / \alpha_1) / \lambda_{\min}(P)} + k_{f2} \|y_{o1}\|_{\infty} + b_{f2} \|\dot{y}_{o1}\|_{\infty} \\
|Z_r| &\leq (k_{r2} + b_{r2}) \sqrt{(V(0) + \beta_1 / \alpha_1) / \lambda_{\min}(P)} + k_{r2} \|y_{o2}\|_{\infty} + b_{r2} \|\dot{y}_{o2}\|_{\infty}
\end{aligned} \quad (35)$$

Hence, we can tune the design parameters η_1, η_2 and P , such that the tire load constraints (2) can be achieved.

Finally, the suspension travel constraints (5) will be studied. The bounds of the suspension spaces can be obtained from the result of Theorem 1, i.e. $-\underline{\delta} \phi_i(t) < x_i(t) < \bar{\delta} \phi_i(t), \forall t > 0$, we know that $|x_1| < \max\{\underline{\delta}, \bar{\delta}\} \phi_{10}$ and $|x_3| < \max\{\underline{\delta}, \bar{\delta}\} \phi_{20}$, which implies that

$$\begin{aligned}
|\Delta y_f| &\leq |x_1| + a |\sin x_3| + |x_5| \leq |x_1| + a |x_3| + |x_5| \\
&\leq \max\{\underline{\delta}, \bar{\delta}\} (\phi_{10} + a \phi_{20}) + \sqrt{(V(0) + \beta_1 / \alpha_1) / \lambda_{\min}(P)}
\end{aligned} \quad (36)$$

$$\begin{aligned}
|\Delta y_r| &\leq |x_1| + b |\sin x_3| + |x_7| \leq |x_1| + b |x_3| + |x_7| \\
&\leq \max\{\underline{\delta}, \bar{\delta}\} (\phi_{10} + b \phi_{20}) + \sqrt{(V(0) + \beta_1 / \alpha_1) / \lambda_{\min}(P)}
\end{aligned} \quad (37)$$

Then we can tune the PPF parameters $\underline{\delta}, \bar{\delta}, \phi_{i0}$ and the design parameters η_1, η_2 and matrix P to guarantee the

suspension travel constraints (5). It should be noted that the parameters η_1 and η_2 are used for analysis only; they are not used in the control implementation. Thus, they can be set very small such that β_1 is small to fulfill (35)-(37).

Remark 5: Compared to generic adaptive control without PPF (as shown in next section), a salient feature of PPF control is that it can guarantee not only the steady-state error bounds but also the transient response of x_1, x_3 . Moreover, the parameters $\underline{\delta}, \bar{\delta}, \phi_{i0}$ can be *a priori* selected to fulfill the initial condition $-\underline{\delta} \phi_i(0) < x_i(0) < \bar{\delta} \phi_i(0)$ as [38]. **In this case, the parameter tuning to fulfill (2) and (5) can be simplified because $\underline{\delta}, \bar{\delta}, \phi_{i0}$ are explicitly shown in (36)-(37).**

Remark 6: In practical applications, the parameters to be set for the proposed PPF control can be grouped into two categories: PPF parameters and feedback control parameters. A parameter tuning guideline can be given as in [25]:

1) **The positive constants $\bar{\delta}, \underline{\delta}$ and $\phi_{i0}, i = 1, 2$ should be chosen to fulfill the initial conditions $-\underline{\delta} \phi_i(0) < x_i(0) < \bar{\delta} \phi_i(0)$.**

The PPF parameter a_i can be set as a tradeoff between the amplitude of the required control forces and the convergence speed of the displacements x_i . The steady-state error bound $\phi_{i\infty}$ can be set large in the initial tuning phase, which can be reduced in the subsequent operation to fulfill performance requirements. In general, small $\phi_{i\infty}$ and large α_i can obtain good control performance but lead to large control action.

2) Large feedback gains k_{p1}, k_{p2} in the control will lead to faster error convergence, whereas the required control action may be aggressive (and oscillatory due to road disturbances). Moreover, high adaptive gains Γ_{p1} and Γ_{p2} can help to improve parameter estimation but may make the control action aggressive. Finally, the leakage constant σ in the adaptive laws (26) and (27) determines the parameter estimation convergence speed, which is also related to the excitation level.

IV COMPARISON WITH OTHER ADAPTIVE CONTROL DESIGNS

To show the advantages of PPF control (21) and the new adaptive law (26), this section will present a generic adaptive controller in combination with various adaptive laws for comparison. For brevity, we only consider the control design for x_1 , while the control of x_3 and the performance analysis of (2) and (5) are not repeated.

We define a filtered error as:

$$s_1 = [\Lambda, 1][x_1, \dot{x}_1]^T \quad (38)$$

where $\Lambda > 0$ is a positive constant [22]. Then, the time derivative of s_1 along (7) is given as:

$$\begin{aligned}
\dot{s}_1 &= \Lambda x_2 + \theta_1 (-F_{df} - F_{dr} - F_{sf} - F_{sr} + u_y + d_1) \\
&= \Lambda x_2 + W_1^T \Phi_1 + \varepsilon_{o1}
\end{aligned} \quad (39)$$

where we use an NN to approximate the unknown dynamics $T_1(Z_1) = \theta_1 (-F_{df} - F_{dr} - F_{sf} - F_{sr}) = w_1^T \phi_1(Z_1) + \varepsilon_1$; the NN weight $w_1 \in R^L$ and the residual error $\varepsilon_{o1} = \varepsilon_1 + \theta_1 d_1$ are bounded

$\|w_1\| \leq w_{1N}, |\varepsilon_{01}| \leq \varepsilon_{01N}$, $\phi_1(Z_1) \in R^L$ is the regressor. Thus, $W_1 = [w_1^T, \theta_1^T]^T$ ($\|W_1\| \leq W_{1N}$) and $\Phi_1 = [\phi_1^T(Z_1), u_y^T]^T$ are the augmented weight and regressor.

The generic adaptive control u_y is given as

$$u_y = \frac{1}{\hat{\theta}_1} [-\hat{w}_1^T \phi_1(Z_1) - k_1 s_1 - \Lambda x_2] \quad (40)$$

where $k_1 > 0$ is the feedback gain, $\hat{\theta}_1$ and \hat{w}_1 are the estimates of θ_1 and w_1 , which will be online updated based on the following adaptive laws for $\hat{W}_1 = [\hat{w}_1^T, \hat{\theta}_1^T]^T$.

Substituting (40) into (39), the control error dynamics are

$$\dot{s}_1 = -k_1 s_1 + \tilde{W}_1^T \Phi_1 + \varepsilon_{01} \quad (41)$$

For adaptive control (40), various adaptive laws have been suggested. Hence, we will present the widely used gradient descent and e -modification schemes and compare them with the adaptive law with a new leakage term as from [27].

A. Gradient Based Adaptive Law [22]

The gradient descent adaptive law is solely driven by the tracking error s_1 as

$$\dot{\hat{W}}_1 = \Gamma_1 s_1 \Phi_1 \quad (42)$$

where $\Gamma_1 > 0$ is the learning gain.

Lemma 4: Consider the suspension system (7) with control (40) and adaptive law (42). If there is no residual error ($\varepsilon_{01} = 0$), then the control error x_1 converges to zero asymptotically.

Proof: Please refer to Appendix III.

For the gradient descent adaptive law (42), the estimation error \tilde{W}_1 may asymptotically converge to zero under the PE condition and the ideal case, $\varepsilon_{01N} = 0$. However, the presence of any disturbances ($\varepsilon_{01N} \neq 0$) may trigger instability of the closed-loop system [22], which makes this adaptive law difficult to use in practice.

B. e -modification Adaptive Law [22]

To address the boundedness of \hat{W}_1 , a forgetting factor is added in (42) to give the e -modification scheme

$$\dot{\hat{W}}_1 = \Gamma_1 s_1 \Phi_1 - \Gamma_1 \sigma |s_1| \hat{W}_1 \quad (43)$$

where $\sigma > 0$ is a positive constant.

Lemma 5: Consider the suspension system (7) with control (40) and adaptive law (43), then x_1 and \tilde{W}_1 will ultimately converge to a small set defined by

$$\Omega = \left\{ \tilde{W}_1, s_1, \|\tilde{W}_1\|, |s_1| \leq \sqrt{2\beta_5 / (\min(k_1, \sigma \lambda_{\min}(\Gamma)), \min(1, \lambda_{\min}(\Gamma^{-1})))} \right\} \text{ for } \beta_5 = \varepsilon_{01N} + \sigma W_{1N}^2 / 2.$$

Proof: Please refer to Appendix IV.

In comparison to the gradient descent method, the e -modification method can guarantee that both \tilde{W}_1 and s_1 are bounded. Thus, the potential bursting phenomenon [22] encountered in the gradient scheme is eliminated. However, since a damping term $\sigma |s_1| \hat{W}_1$ is used in (43), it is shown in

Lemma 5 that the ultimate bounds of x_1 and \tilde{W}_1 depend not only on the error ε_{01} but also on the unknown NN weight bound W_{1N} . Thus, the convergence of x_1 and \tilde{W}_1 to zero cannot be achieved even when $\varepsilon_1 = 0$ and $d_1 = 0$.

C. New Adaptive Law with Estimation Error

To guarantee parameter estimation convergence, we will propose a new adaptive law using the idea shown in Section III. Define the filtered variables $s_{1f}, \Phi_{1f}, x_{2f}$ in system (39) and auxiliary matrix P_1 and vector Q_1 as:

$$\begin{cases} k\dot{s}_{1f} + s_{1f} = s_1, & s_{1f}(0) = 0 \\ k\dot{\Phi}_{1f} + \Phi_{1f} = \Phi_1, & \Phi_{1f}(0) = 0 \\ k\dot{x}_{2f} + x_{2f} = x_2, & x_{2f}(0) = 0 \end{cases} \quad (44)$$

and

$$\begin{cases} \dot{P}_1 = -lP_1 + \Phi_{1f}\Phi_{1f}^T, & P_1(0) = 0 \\ \dot{Q}_1 = -lQ_1 + \Phi_{1f}[(s_1 - s_{1f})/k - \Lambda x_{2f}], & Q_1(0) = 0 \end{cases} \quad (45)$$

where $k > 0$, $l > 0$ are the design parameters.

Then, a new leakage term H_1 can be obtained as

$$H_1 = P_1 \hat{W}_1 - Q_1. \quad (46)$$

The adaptive law for updating \hat{W}_1 is given by:

$$\dot{\hat{W}}_1 = \Gamma_1 s_1 \Phi_1 - \Gamma_1 \sigma H_1. \quad (47)$$

Similar to (55)-(57), one can obtain that $H_1 = -P_1 \tilde{W}_1 + \Delta_1$,

where $\Delta_1 = -\int_0^t e^{-l(t-r)} \Phi_{1f}(r) \varepsilon_{01f}(r) dr$ is bounded by $|\Delta_1| \leq \varepsilon_{1Nf}$ and ε_{01f} is given by $k\dot{\varepsilon}_{01f} + \varepsilon_{01f} = \varepsilon_{01}$.

Lemma 6: Consider the suspension system (7) with control (40) and adaptive law (47), if $\lambda_{\min}(P_1) > \sigma_1 > 0$ (i.e. Φ_1 is PE), then the errors x_1 and \tilde{W}_1 will ultimately satisfy

$$|x_1| \leq \sqrt{\eta(\varepsilon_{01N}^2 + \sigma \varepsilon_{1Nf}^2) / \tilde{\mu}_1 \Lambda}, \quad \|\tilde{W}_1\| \leq \sqrt{\eta(\varepsilon_{01N}^2 + \sigma \varepsilon_{1Nf}^2) / \tilde{\mu}_1 \lambda_{\min}(\Gamma_1^{-1})},$$

which is zero if there is no residual error ($\varepsilon_{01N}, \varepsilon_{1Nf} = 0$).

Proof: Please refer to Appendix V.

It is shown in Lemma 6, that the ultimate bounds of \tilde{W}_1 and x_1 depend on the residual error ε_{01N} , ε_{1Nf} only. Hence, without disturbance ($d_1 = 0$), the errors x_1 and \tilde{W}_1 can be made arbitrarily small if the number of NN nodes L is sufficiently large [39], although there is no generic method to calculate the exact value of ε_{01N} . Nevertheless, in the ideal case when the residual error is zero, i.e. $\varepsilon_{01N} = 0$, the control and estimation errors (e.g. x_1 , \tilde{W}_1) will converge to zero. Thus, the new adaptive law (47) can guarantee better convergence of \tilde{W}_1 and s_1 in comparison to the e -modification (43), which will be shown in simulation.

Remark 7: The design of adaptive laws (26) and (47) with new leakage terms is inspired by our previous work [27, 28]. However, an essential difference is that we consider the tracking error equations (22) and (41) rather than the original system equation in [27, 28] because the unknown parameters are involved in (26) and (47) rather than (7).

D. Summary

We will compare both the control and parameter estimation performances of these four different control schemes:

- i) The proposed PPF control (21) with (26);
- ii) Generic adaptive control (40) with gradient scheme (42);
- iii) Generic adaptive control (40) with e -modification (43);
- iv) Generic adaptive control (40) with new adaptive law (47).

The main conclusions are summarized in Table I and presented in the follows with more detailed explanations.

1) Control performance: It is shown in Theorem 1 that both the transient and steady-state bounds of x_1 can be guaranteed by PPF control (21). However, for generic adaptive control (40) with gradient scheme (42), e -modification (43) and the novel adaptive law (47), the transient response cannot be guaranteed although the steady-state performance may be proved as stated in Lemma 4- Lemma 6. It is known that the ride comfort and safety of vehicle systems can be severely affected by a poor transient suspension response. In this sense, the PPF control provides better suspension profiles among all these approaches. This fact will be validated in simulations.

2) Parameter estimation: For the gradient descent scheme (42), the convergence of the estimated parameters is guaranteed only if the residual error $\varepsilon_{OIN} = 0$ and the PE condition holds, which may be stringent in practice. With the e -modification in (43), only the boundedness of the estimates can be proved, where the bound of the estimation error \tilde{W}_1 depends on the bound of the unknown NN weight W_1 as shown in Lemma 5; this bound may be large even in the absence of the NN approximation error. In contrast, the inclusion of novel leakage terms σH_{p1} in (26) and σH_1 in (47) guarantees that the ultimate bound of \tilde{W}_1 depends only on the residual errors ε_{1Nf} and ε_{OIN} , and thus it can be sufficiently small for large design parameters L , k_1, σ , Γ_1 and for $d_1 = 0$. In the ideal case when $\varepsilon_{OIN} = 0$, we know \tilde{W}_1 converges to zero exponentially, i.e. $\tilde{W}_1 \rightarrow 0$. **Based on the certainty equivalence principle in [22], better control response can be achieved. This point will also be validated in terms of simulations in Section VI.**

TABLE I SUMMARIZATION OF VARIOUS METHODS

Methods	Transient bound	Steady-state bound	Parameter convergence ($\varepsilon_{1N} \neq 0$)	Parameter convergence ($\varepsilon_{1N} = 0$)
PPF control (21) & new adaptation (26)	Yes	Yes	Bounded	Exponential
Control (40) & gradient (42)	No	No	No	Asymptotic
Control (40) & e -modification (43)	No	Yes	Bounded	Bounded
Control (40) & new adaptation (47)	No	Yes	Bounded	Exponential

V CONSIDERATION OF ACTUATOR DYNAMICS AND SATURATION

It is well-known that the actuator is a key component in

active suspension systems, which is used to create the required forces to reduce the uninterrupted effect of road roughness. To address practical implementation of the proposed methods, this section will further consider the actuator dynamics and also potential saturation problems [40-42] due to the constraints imposed on the actuators. The modified control structure can be found in Fig.2.

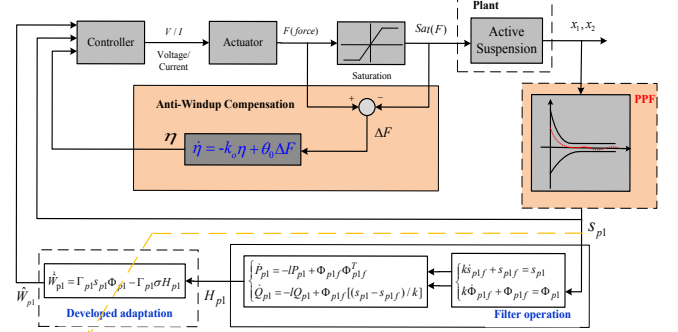


Fig.2 Control system with anti-windup compensation

In this study, electrical linear motors are used as the actuators to realize the active suspension system. This linear servo motor has been practically used in a realistic suspension test-rig [14], where the input voltages can be manipulated to generate the required forces. We refer to [14] for more detail of modeling this actuator. Here, without considering the trivial motor inherent time-delay (4ms), we use a transfer

function $\frac{F}{V} = \frac{100728}{s + 320.4019}$ to represent the relationship

between the input voltage V and the output force F .

Moreover, an anti-windup approach as used in [40] is incorporated into the proposed controller to handle the potential control saturation problem when the actuators suffer from input constraints. Here, we only show the modifications of the PPF control u_y with anti-windup. The design of u_φ is similar to that of u_y , which will not be repeated.

The basic idea of this anti-windup design is to construct an augmented controller, which matches the predefined one when the saturation does not occur, and guarantees feasible performance degradation when the saturation occurs [41, 42]. This can be achieved by modifying the control actions when the control actions are saturated. This anti-windup scheme is a simplified version of the low order structures suggested in [41, 42]. The compensator can be given as follows

$$\dot{\eta}_1 = -k_{o1}\eta_1 + \theta_0 \Delta F \quad (48)$$

where k_o, θ_0 are positive constants and $\Delta F = u_y - \text{sat}(u_y)$ with $\text{sat}(\cdot)$ being a saturation function [41, 42].

Then the PPF control (21) is altered as

$$u_y = \frac{1}{\tau_1 \hat{\theta}_1} [-k_{p1} s_{p1} - \hat{w}_{p1}^T \phi_{p1}(Z_{p1}) + k_{o1} \eta_1] \quad (49)$$

It is noted that η_1 in (48) is used to compensate for the error s_{p1} in (49) when $\Delta F \neq 0$. It can be taken as a low-pass filter version of ΔF . When the control input is small (i.e. $\Delta F = 0$), η_1 is kept at 0, thus the convergence and the closed-loop system stability is preserved as in the

unsaturated case. When the saturation occurs, η_1 can help to reshape the control action u_y so as to drive the controller back into the linear region of the saturation [41, 42]. This is summarized for the simplified case where the actuator dynamics are neglected, i.e. $F/V=1$

Theorem 2: Consider $F/V=1$, the vertical displacement x_1 in the suspension system (7) and the modified PPF control (49). If the initial condition fulfills $-\delta\varphi_1(0) < x_1(0) < \bar{\delta}\varphi_1(0)$, and the regressor vector Φ_{p1} in (49) is PE for small disturbance and residual NN error, then

- 1) For small enough initial values (i.e. there is no saturation, $\Delta F_y = 0$), the closed-loop system is the same within a compact set as for Theorem 1, and the conclusions of Theorem 1 still hold;
- 2) When $\Delta F_y \neq 0$, the control error s_{p1} is bounded in a local sense, which guarantees PPF control performance.

Proof [40]: Please refer to Appendix VI.

The simulations show that the suspension performance can be maintained with less degradation compared to the case without anti-windup compensator. The case of $F/V \neq 1$ is investigated in simulation only for space reasons.

VI SIMULATIONS

In this section, simulations are provided to exemplify the effectiveness of the proposed controllers and the novel adaptive laws. To provide realistic conditions, a commercial vehicle simulation software Carsim® (Version 8.1) is used together with Matlab® Simulink (2014a) to build a combined dynamic simulator. The schematic of the built simulation system is shown in Fig.3, where realistic driving maneuvers and the associated road profiles (e.g. bounce sine sweep road) embedded in Carsim are imported into Simulink as the road disturbance to test the active suspension control systems.

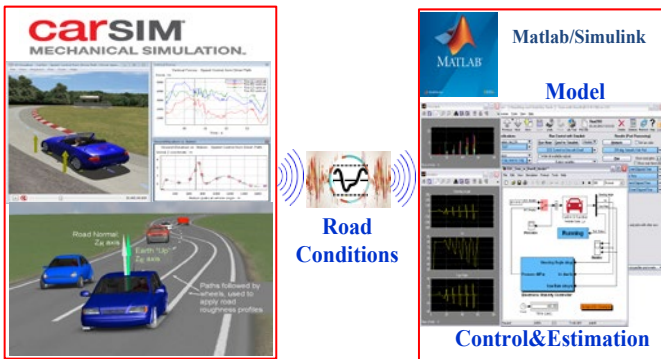


Fig.3 Schematic of dynamic simulation system.

In the simulations, the unknown forces of the nonlinear stiffening springs, piece-wise dampers and the tire obey are given in [21] as :

$$F_{sf} = k_{f1}\Delta y_f + k_{nf1}\Delta y_f^3, F_{sr} = k_{r1}\Delta y_r + k_{nr1}\Delta y_r^3 \quad (50)$$

$$F_{df} = b_c\Delta \dot{y}_f, F_{dr} = b_e\Delta \dot{y}_r \quad (51)$$

$$F_{tf} = k_{f2}(y_1 - y_{o1}), F_{tr} = k_{r2}(y_2 - y_{o2}) \quad (52)$$

$$F_{bf} = b_{f2}(\dot{y}_1 - \dot{y}_{o1}), F_{br} = b_{r2}(\dot{y}_2 - \dot{y}_{o2}) \quad (53)$$

where k_{f1}, k_{r1} and k_{nf1}, k_{nr1} are the stiffness coefficients of the linear and nonlinear terms; b_{ei} and b_{ci} ($i=1,2$) are the damping coefficients for the extension and compression movements; k_{f2}, k_{r2}, b_{f2} and b_{r2} are the stiffness and damping coefficients of the tire. The parameters of the half-car model shown in Fig.1 are the same as those used in [21], which are listed in TABLE II.

TABLE II PARAMETERS FOR HALF-CAR MODEL

Parameter	Value	Parameter	Value
M	1200 kg	k_{r2}	200,000 N/m
I	600 kgm ²	b_{f2}	1500 Ns/m
m_f	100 kg	b_e	1500 Ns/m
m_r	100 kg	b_{r2}	2000 Ns/m
k_{f1}	15,000 N/m	b_c	1200 Ns/m
k_{r1}	15,000 N/m	a	1.2 m
k_{nf1}	1000 N/m	b	1.5 m
k_{nr1}	1000 N/m	V	20 km/h
k_{f2}	200,000 N/m	l_b	2.5 m

Then the following three cases are studied and compared.

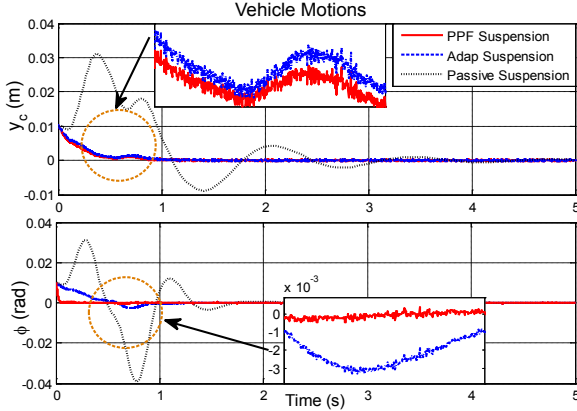
Case 1 (Bump disturbance): The following benchmark bump-type road disturbance has been widely used (e.g.[21]) to test the performance of suspension systems:

$$y_{o1}(t) = \begin{cases} \frac{h}{2} \left(1 - \cos\left(\frac{2\pi V}{l_b} t\right)\right) & 0 \leq t \leq \frac{l_b}{V_s} \\ 0 & t > \frac{l_b}{V_s} \end{cases} \quad (54)$$

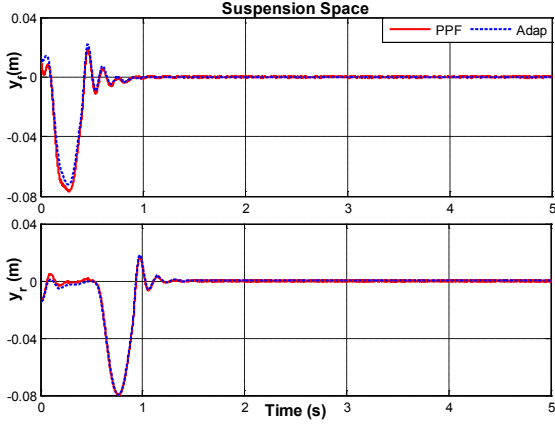
The road input y_{o2} for the rear tire is implemented as $y_{o2}(t) = y_{o1}(t - \tau)$ where the delay $\tau = 0.5$ sec is calculated based on the vehicle velocity V_s and the length of the bump l_b ; $h = 0.08$ m is the height of the bump.

The effectiveness of the proposed PPF control (21) is compared with generic adaptive control (40) for the initial values $x_i(0) = 0, i=2,4,6,8$ and $x_i(0) = 0.01$ m, $i=1,5,7$, $x_3(0) = 0.01$ rad, $\theta_1(0) = 1/1000, \theta_2(0) = 1/500$. The PPFs are chosen as $\varphi_1(t) = (0.02 - 0.005)e^{-7t} + 0.005$, $\varphi_2(t) = (0.02 - 0.005)e^{-9t} + 0.005$ with $\bar{\delta} = \underline{\delta} = 1$, and other simulation parameters of PPF control (21) and adaptive law (26) are set as $k_{p1} = 120, k_{p2} = 105, \Lambda_{p1} = 5, \Lambda_{p2} = 8, k = 0.001, l = 1, \sigma = 0.01$, and the adaptive gains $\Gamma_{p1} = 50 \text{diag}[2.4, 3.9, 1000, 10120, 270, 3250, 1.6e^{-10}]$ and $\Gamma_{p2} = 50 \text{diag}[2.2, 1270, 13500, 1.6, 300, 2070, 2.35e^{-10}]$. **To show the effect of sensor noise, a band-limited white noise was manually added to the measured displacements to test the robustness of the proposed control in this case study.** The generic adaptive control (40) with the new adaptive law (47) is also simulated, where the parameters are set as $k_1 = 130, k_2 = 150, \Lambda_1 = \Lambda_2 = 5, k = 0.001, l = 1, \sigma = 5$, and the gains are $\Gamma_1 = 30 \text{diag}[3.35, 4.85, 1200, 11050, 420, 3960, 7e^{-8}]$ and

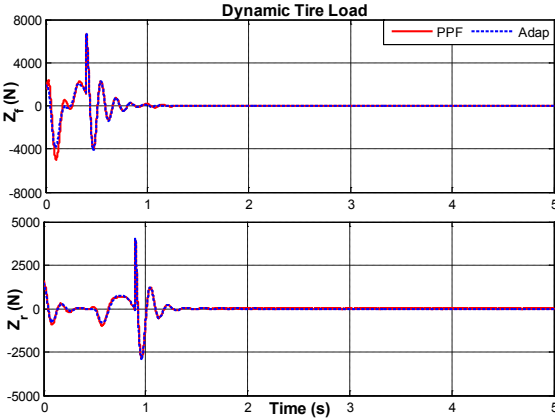
$$\Gamma_2 = 30 \text{diag}[3.6, 1270, 12600, 2.1, 320, 2700, 7e^{-8}].$$



(a) Vehicle motions with/without active suspension



(b) Suspension travels of front and rear wheels



(c) Dynamic tire loads of front and rear wheels

Fig.4 Vehicle responses with/without active suspension. (PPF: PPF control (21); Adap: generic adaptive control (40)).

Fig.4(a) shows the time response of the vertical and pitch displacements with the PPF control (21), adaptive control (40), and passive suspension (i.e. the active controls are turned off). One can find from Fig. 4(a) that these two active control approaches are able to isolate the road disturbance effectively to regulate the vertical and pitch displacements to zero rapidly **even in the presence of sensor noise. Hence, the effect of sensor noise can be diminished.** Moreover, the PPF control (21) has faster transient convergence speed than the generic adaptive control (40). In Fig. 4(b)-(c), it is also shown that the suspension travels and tire loads are all within the

allowable ranges even for a harsh bump road disturbance. One may find that the PPF control has slightly higher peaks in both the suspension travels and tire loads than that of generic adaptive control in the transient stage. This is reasonable because the ride comfort, suspension travel and tire loads are conflicting in the active suspension. Thus, the PPF control method that provides better ride comfort requires larger suspension travels and tire loads.

Moreover, to show the effects of the novel leakage terms $\sigma H_1, \sigma H_2$ on the parameter estimation convergence, generic adaptive control (40) is simulated with the classical gradient descent scheme (42), the e -modification method (43) and the new adaptive law (47), respectively. We verified that the PE condition can be guaranteed for this bump road disturbance by testing the condition $\lambda_{\min}(P_{p1}), \lambda_{\min}(P_{p2}) > 0$, which is needed for parameter estimation convergence. The estimation performance of these three schemes is compared. Fig.5 shows that the estimated parameters with the new adaptive law (47) converge to their true values. In particular, the estimation of the unknown mass θ_1 and the moment of inertia θ_2 shown in Fig.5 can be precisely estimated with the help of the novel leakage terms. However, the gradient and e -modification adaptive laws cannot guarantee the error convergence. As analyzed in Section IV, the ultimate bound of the parameter estimation error \tilde{W}_1 with e -modification depends not only on the bound of residual NN error ε_{1N} , but also on the bound of ideal NN weight W_{1N} . Hence, the estimated parameters with the e -modification only stay in a bounded set around the pre-selected values rather than converge to their true values. This has been significantly improved by using the proposed adaptive laws.

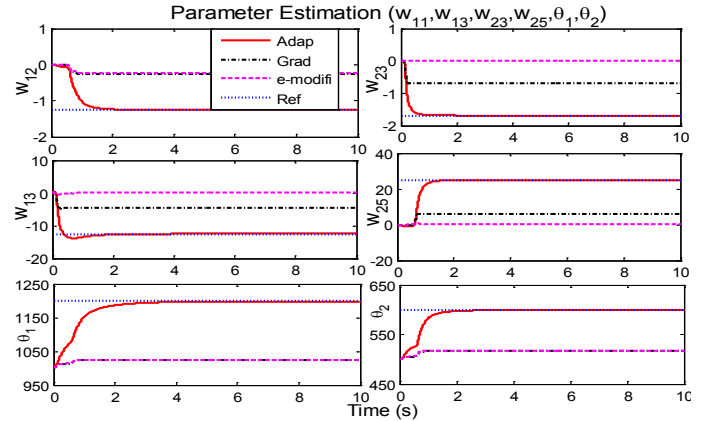


Fig.5 Comparative parameter estimation performances (Ref: reference; Adap: new adaptive law (47); Grad: gradient descent scheme (42), e-modifi: e -modification method (43)).

Case 2 (Bounce Sine Sweep road disturbance): To validate the proposed methods in more realistic driving maneuvers, a typical driving road profile configured in Carsim (i.e. bounce sine sweep road condition (sinusoidal with varying frequency) with the vehicle driving velocity as 40km/h) is generated and used to test the performance of active suspension controls. Fig.6(a) shows the ground elevation of the test road.

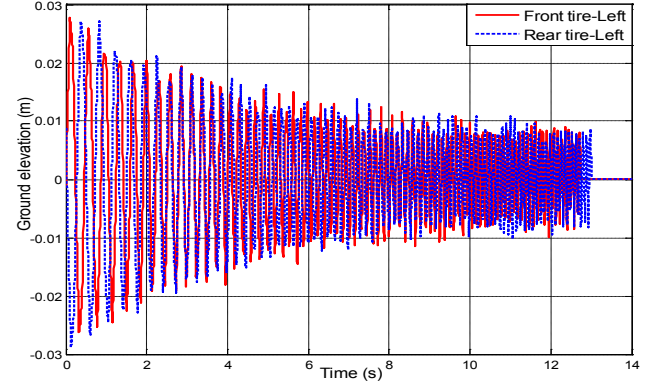
In this case, the initial values and the parameters of generic adaptive control are chosen as the ones in Case 1, while the PPFs can be set as $\varphi_1(t) = (0.012 - 0.0002)e^{-10t} + 0.0002$ and $\varphi_2(t) = (0.012 - 0.00035)e^{-10t} + 0.00035$ to achieve better transient suspension performance. Simulation results in terms of time-domain responses are provided in Fig. 6, where the PPF control (21) with (26) is compared with the generic adaptive control (40) with the gradient method (42) and with the new adaptation (47). As shown in Fig. 6(b), the proposed PPF control (21) can obtain better regulation performance of both the vertical and pitch displacements than adaptive control (40) without the PPF. Especially, the transient response of $x_i, i=1,3$ with the PPF control (21) can be strictly retained within the predefined bounds. However, the generic adaptive control (40) with conventional adaptive laws (42) and (43) provide a sluggish transient response because the precise estimation of unknown parameters cannot be obtained. Moreover, the use of the new adaptation law (47) can lead to better estimation than that of the gradient descent scheme (42). In fact, similar parameter estimation to Fig.5 can be obtained with the new adaptive laws (47). Therefore, from the certainty equivalence principle in [22], better control response can be achieved with the suggested adaptive laws, which has been shown in Fig.6(b). This simulation clearly indicates how the use of the new leakage terms with the estimation error and the PPFs can improve the estimation and thus control performance.

Moreover, considering the strictly limited working space in the suspension system, Fig.6(c) shows that the suspension travels with different controllers are all smaller than the standard limitations $\Delta y_{f \max} = 0.08m$, $\Delta y_{r \max} = 0.08m$. Finally, to ensure the car safety, the dynamic tire loads must be ensured to retain the suspension performance constraint (2). As shown in Fig.6(d), both the front and rear wheel static tire loads can be calculated by (3) as $F_f < 7513.3N$, $F_r < 6206.7N$, where the responses and peaks of dynamic tire loads for two wheels are limited within these specific bounds. Overall, in spite of different transient suspension response of the vertical and pitch displacements, all these three control approaches can retain these suspension requirements.

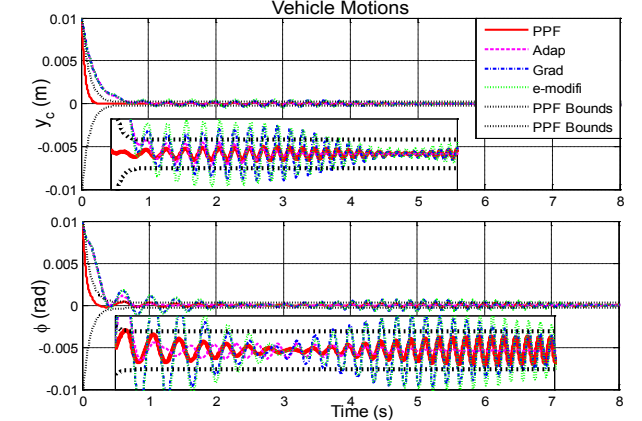
To further validate the proposed control methods, frequency-domain analysis are also considered. For further comparison, the classical 2-states skyhook control (SH 2-States) method [43] is implemented and compared with the proposed methods in the frequency domain. The frequency responses of different methods can be shown in Fig.6(e), where the performance index, Power Spectral Density (PSD), is introduced to evaluate the effectiveness of these methods. It is clearly shown that the active suspension controls can achieve better response than passive suspension and skyhook control. Moreover, it can also be found that the proposed adaptive control method (40) with novel adaptive law (47) achieves the lower peak values than that with e-modification (43) over the resonant frequency range 4-8Hz, which is sensitive to human body. This again implies that the estimated parameter convergence can indeed help to improve the

suspension responses and ride comfort. Nevertheless, it is interesting to find that the PPF control achieves higher PSD values than the e -modification method around 8 Hz. This is reasonable because it achieves the fastest transient convergence speed compared with that of other control methods in the time-domain (Fig.6(b)), while its frequency response around some specific frequencies (e.g. 8 Hz) may be degraded.

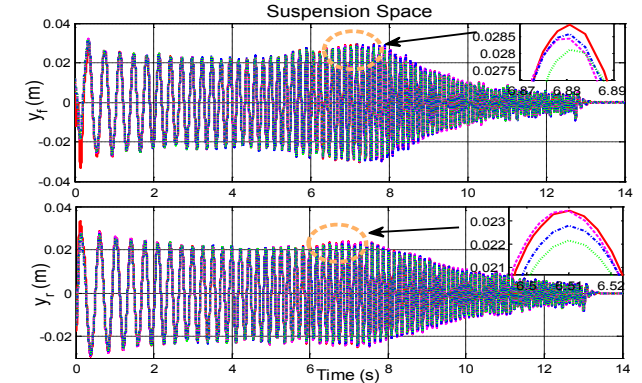
Finally, the improved ride comfort can also be observed in terms of another performance index, root mean square (RMS) of acceleration, which has been shown in Fig.6 (f). It is also shown that the proposed adaptive control (40) and PPF control (21) can yield smaller Root Mean Square (RMS) values than other methods. This further verifies the effectiveness and feasibility of the proposed methods.



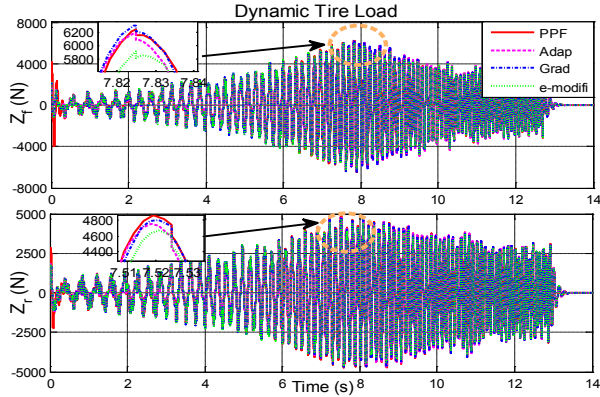
(a) Ground road elevation of bounce sine sweep.



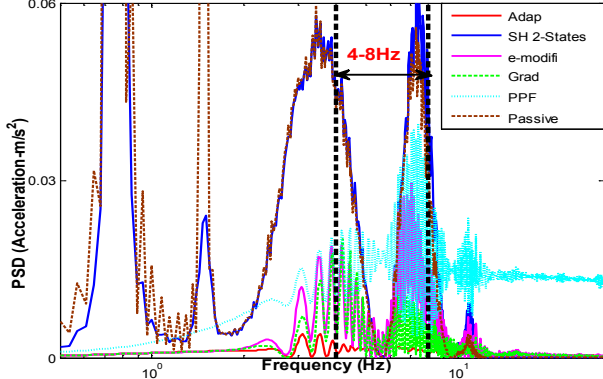
(b) Vehicle suspension motions with bounce sine sweep.



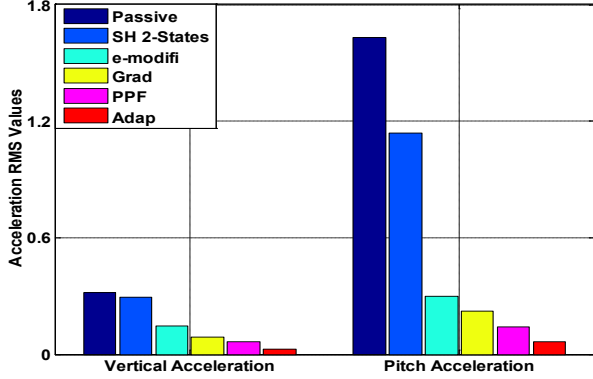
(c) Suspension travels of the front and rear wheels.



(d) Dynamic tire loads of the front and rear wheels.



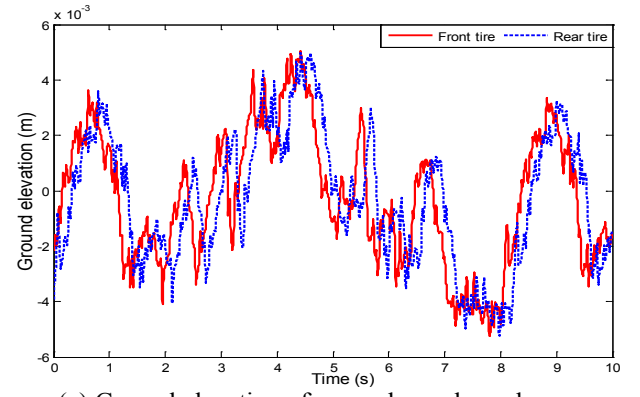
(e) Frequency domain analysis for different methods



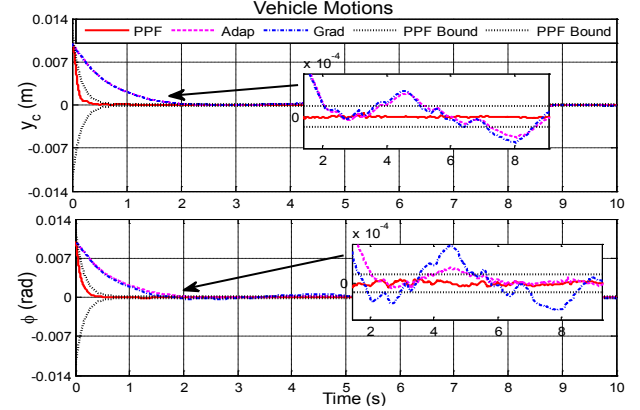
(f) Acceleration RMS values for different methods

Fig.6 Simulation results with bounce sine sweep road disturbance. (PPF: PPF control (21) with (26); **Adap**: adaptive control (40) with (47); Grad: adaptive control (40) with (42), e-modifi: adaptive control (40) with (43)).

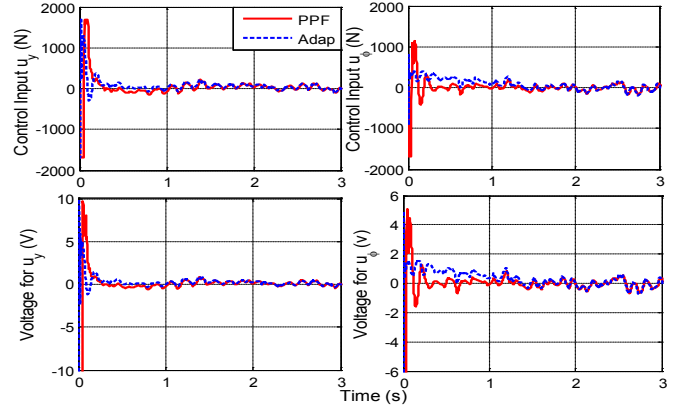
Case 3 (Straight lane with example road roughness): Finally, we choose the driving road as a straight lane with road roughness embedded in Carsim and the vehicle traveling at 60km/h . The ground elevation is plotted in Fig.7(a). In this case, the actuator dynamics and saturation (e.g. servo motor described in Section V) are all considered and the proposed anti-windup compensators are implemented. Thus, the PPF is set as $\varphi_1(t) = \varphi_2(t) = (0.013 - 0.00015)e^{-9t} + 0.00015$ and the other parameters are set $\Lambda_{p1} = \Lambda_{p2} = 2, k_{p1} = 0.5, k_{p2} = 1$. The parameters for the actuator saturation and anti-windup compensator are $k_o = 0.05, u_{y\max} = u_{z\max} = 1700\text{N}$. These parameters are tuned based on the guidelines provided in Remark 6.



(a) Ground elevation of example road roughness.



(b) Vehicle motions with different control methods.



(c) Response of control forces and voltages for motors

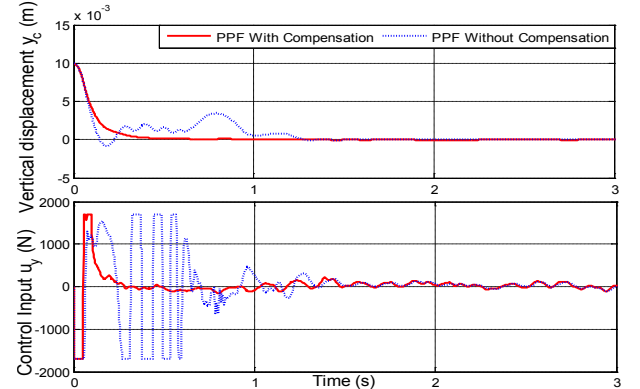
(d) Displacement and control u_y with/without anti-windup

Fig.7 Simulation results with example road roughness (PPF: PPF control (21) with (26); **Adap**: adaptive control (40) with (47); Grad: adaptive control (40) with (42)).

Comparative simulation results are provided in Fig.7, where the performance of the active suspension system with different methods are illustrated. One can find from Fig.7(b) that the proposed PPF control can obtain best control performance for both the vertical and angular displacements due to the use of PPF scheme. Specifically, it is shown that not only faster transient convergence speed is achieved in comparison to these general adaptive controls without PPF, but also smaller steady-state error is guaranteed, i.e. $x_i, i = 1, 3$ can be strictly retained within the prescribed PPF bounds.

The profiles of the required forces u_y, u_ϕ and the corresponding input voltages for the motors (that are used to generate the required forces) are plotted in Fig.7(c). One may find from the top figures of Fig.7(c) that the required forces and the control voltage are all bounded. In particular, the control voltages for the motors are all retained within $[-10, +10]$ V. Thus, the proposed control methods can be practically implemented. Moreover, in Fig.7(c), it is also illustrated that **the forces of the PPF control has higher peaks in the first few seconds than generic adaptive control without PPF**. This is reasonable because **larger control forces should be used to achieve faster control convergence during the transient**; this is particularly true if the initial errors are significant.

The effectiveness of the anti-windup compensator for vertical motion and the corresponding control signal is also demonstrated in Fig.7(d). One may find from the top subfigure of Fig.7(d) that the PPF control with the anti-windup compensator can regulate the vertical displacement to zero faster and smoother than the PPF control without the anti-windup compensator. This can be explained by observing the control signals as depicted in the bottom subfigure of Fig.7(d), where it is shown that the proposed anti-windup compensator can effectively address the saturation problem, i.e. it can drive the control signals and the closed-loop system back to a stable region, even when the actuators are subject to control constraints (the maximum forces are saturated by 1700N in this case). A similar result can also be observed for the PPF control for pitch motion, which is not shown here due the page limit.

VII CONCLUSION

In this paper, an alternative adaptive control based on new adaptive laws is proposed for vehicle active suspension systems with unknown nonlinear sprung and damper dynamics. Both the transient and steady-state control performance of the vertical and angular displacements can be guaranteed by introducing a prescribed performance function and the associated error transform. A new adaptive law based on the parameter estimation error is also used such that precise estimation of essential vehicle parameters is achieved. The suggested new leakage terms can be superimposed on the classical gradient descent method to achieve better estimation and control performance. Extensive comparisons to generic adaptive control with well-known adaptations (e.g. gradient, e -modification) are carried out. The suspension requirements concerning the ride comfort and vehicle safety are all studied. Comparative simulations on a half-car model in a dynamic

simulator consisting of Carsim[®] and Matlab[®]/Simulink are given to validate the effectiveness of the proposed PPF control and new adaptive laws.

Appendix I-Proof of Lemma 2

Proof: By applying a filter operation $(\cdot)_f = (\cdot)/(ks+1)$ on both sides of (22) and considering (23), one can deduce that

$$\dot{s}_{p1f} = \frac{s_{p1} - s_{p1f}}{k} = W_{p1}^T \Phi_{p1f} + \varepsilon_{p1f} \quad (55)$$

where ε_{p1f} is the filtered version of the error ε_{p1} given by $k\dot{\varepsilon}_{p1f} + \varepsilon_{p1f} = \varepsilon_{p1}$, so that ε_{p1f} is also bounded.

On the other hand, one can obtain the solution of the matrix differential equation (24) as

$$\begin{cases} P_{p1} = \int_0^t e^{-l(t-r)} \Phi_{p1f}(r) \Phi_{p1f}^T(r) dr \\ Q_{p1} = \int_0^t e^{-l(t-r)} \Phi_{p1f}(r) [(s_{p1}(r) - s_{p1f}(r)) / k] dr \end{cases} \quad (56)$$

Then from (25)~(56), we can obtain

$$H_{p1} = P_{p1} \hat{W}_{p1} - Q_{p1} = -P_{p1} \tilde{W}_{p1} + \Delta_{p1} \quad (57)$$

where $\Delta_{p1} = -\int_0^t e^{-l(t-r)} \Phi_{p1f}(r) \varepsilon_{p1f}(r) dr$ is a bounded variable because the NN regressor Φ_{p1f} and error ε_{p1f} are bounded, i.e. $\|\Delta_{p1}\| < \varepsilon_{p1Nf}$ holds for a positive constant ε_{p1Nf} . \square

Appendix II-Proof of Theorem 1

Proof: Substituting (21) into (20), we get the control error as

$$\dot{s}_{p1} = \tilde{W}_{p1}^T \Phi_{p1} - k_{p1} s_{p1} + \varepsilon_{p1} \quad (58)$$

Choose a Lyapunov function as

$$V_{p1} = \frac{1}{2} s_{p1}^2 + \frac{1}{2} \tilde{W}_{p1}^T \Gamma_{p1}^{-1} \tilde{W}_{p1} \quad (59)$$

By using $ab \leq a^2 \eta_{p1} / 2 + b^2 / 2 \eta_{p1}$, $\eta_{p1} > 0$, then \dot{V}_{p1} can be calculated along (26) and (58) as

$$\begin{aligned} \dot{V}_{p1} &= -k_{p1} s_{p1}^2 + s_{p1} \varepsilon_{p1} - \sigma \tilde{W}_{p1}^T P_{p1} \tilde{W}_{p1} + \sigma \tilde{W}_{p1}^T \Delta_{p1} \\ &\leq -(k_{p1} - \frac{1}{2\eta_{p1}}) s_{p1}^2 - \sigma (\sigma_{p1} - \frac{1}{2\eta_{p1}}) \|\tilde{W}_{p1}\|^2 + \frac{\eta_{p1}}{2} (\varepsilon_{p1N}^2 + \sigma \varepsilon_{p1Nf}^2) \quad (60) \\ &\leq -\tilde{\mu}_{p1} V_{p1} + \gamma_{p1} \end{aligned}$$

where $\tilde{\mu}_{p1} = \min\{2(k_{p1} - 1/2\eta_{p1}), 2\sigma(\sigma_{p1} - 1/2\eta_{p1}) / \lambda_{\max}(\Gamma_{p1}^{-1})\}$ and $\gamma_{p1} = \eta_{p1}(\varepsilon_{p1N}^2 + \sigma \varepsilon_{p1Nf}^2) / 2$ are all positive constants for appropriately designed parameters k_{p1}, η_{p1} such that $k_{p1} > 1/2\eta_{p1}$ and $\eta_{p1} > 1/2\sigma_{p1}$.

1) In the case when there is no residual error, i.e. $\varepsilon_{p1} = 0$ and $\Delta_{p1} = 0$, one can verify that $\gamma_{p1} = 0$, then (60) is reduced to $\dot{V}_{p1} \leq -\tilde{\mu}_{p1} V_{p1}$. Then according to Lyapunov Theorem, the control error s_{p1} and estimation error \tilde{W}_{p1} converge to zero exponentially.

2) In the case when $\varepsilon_{p1} \neq 0$ and $\gamma_{p1} \neq 0$, according to the Lyapunov's theorem, we know from (60) that V_{p1} and thus s_{p1}, \tilde{W}_{p1} are uniformly ultimately bounded. Moreover, it follows $V_{p1}(t) \leq (V_{p1}(0) - \gamma_{p1} / \tilde{\mu}_{p1}) e^{-\tilde{\mu}_{p1} t} + \gamma_{p1} / \tilde{\mu}_{p1}$, so that s_{p1}

and \tilde{W}_{p1} will converge to the compact set defined by

$$\Omega = \left\{ \tilde{W}_{p1}, s_{p1} \mid \|\tilde{W}_{p1}\| \leq \sqrt{\frac{\eta_{p1}(\varepsilon_{p1N}^2 + \sigma\varepsilon_{p1Nf}^2)}{\tilde{\mu}_{p1}\lambda_{\min}(\Gamma_{p1}^{-1})}}, |s_{p1}| \leq \sqrt{\frac{\eta_{p1}(\varepsilon_{p1N}^2 + \sigma\varepsilon_{p1Nf}^2)}{\tilde{\mu}_{p1}}} \right\}.$$

In both aforementioned cases, the transformed error z_1, \dot{z}_1 and the control input u_y are bounded. Hence, from Lemma 1 and the properties of function $S(z_1)$, we know that $-\underline{\delta} < S(z_1) < \bar{\delta}$ is true. This further implies the condition $-\delta\varphi_1(t) < x_1(t) < \bar{\delta}\varphi_1(t)$ holds based on (11). Then, one can conclude that the control of system (1) with prescribed bound (10) is achieved. \square

Appendix III-Proof of Lemma 4

Proof: We select a Lyapunov function as

$$V_1 = \frac{1}{2}s_1^2 + \frac{1}{2}\tilde{W}_1^T \Gamma_1^{-1} \tilde{W}_1 \quad (61)$$

If the residual error bound $\varepsilon_{01N} = 0$, then \dot{V}_1 can be computed along (41) and (42) as

$$\dot{V}_1 = s_1(-k_1 s_1 + \tilde{W}_1^T \Phi_1) - \tilde{W}_1^T s_1 \Phi_1 \leq -k_1 s_1^2. \quad (62)$$

Then based on the Barbalat's lemma [22], s_1 and thus x_1 will converge to zero asymptotically. \square

Appendix IV-Proof of Lemma 5

Proof: Select a Lyapunov function as (61), then \dot{V}_1 can be computed along (41) and (43) as

$$\dot{V}_1 = -k_1 s_1^2 + s_1 \varepsilon_{01} + \sigma |s_1| \tilde{W}_1^T \hat{W}_1. \quad (63)$$

Consider the fact $\tilde{W}_1^T \hat{W}_1 \leq -\frac{1}{2}\|\tilde{W}_1\|^2 + \frac{1}{2}W_{1N}^2$, then

$$\dot{V}_1 \leq -|s_1| \left[k_1 |s_1| + \frac{\sigma}{2} \|\tilde{W}_1\|^2 - \varepsilon_{01N} - \frac{\sigma}{2} W_{1N}^2 \right] \quad (64)$$

According to the extended Lyapunov Theorem [22], the errors s_1, \tilde{W}_1 converge to the bound defined in Lemma 5. \square

Appendix V-Proof of Lemma 6

Proof: Select a Lyapunov function as (61), then \dot{V}_1 can be computed along (41) and (47) as

$$\begin{aligned} \dot{V}_1 &\leq -(k_1 - \frac{1}{2\eta})s_1^2 - \sigma(\sigma_1 - \frac{1}{2\eta})\|\tilde{W}_1\|^2 + \frac{\eta}{2}\varepsilon_{01N}^2 + \frac{\sigma\eta}{2}\varepsilon_{1Nf}^2 \\ &\leq -\tilde{\mu}_1 V_1 + \gamma_1 \end{aligned} \quad (65)$$

where $\tilde{\mu}_1 = \min\{2(k_1 - 1/2\eta), 2\sigma(\sigma_1 - 1/2\eta)/\lambda_{\max}(\Gamma_1^{-1})\}$ and $\gamma_1 = \eta(\varepsilon_{01N}^2 + \sigma\varepsilon_{1Nf}^2)/2$ are all positive constants for $k_1 > 1/2\eta$ and $\eta > 1/2\sigma_1$. Then, s_1 and \tilde{W}_1 converge to the sets defined in Lemma 6. \square

Appendix VI-Proof of Theorem 2

Proof: Let's assume that for a sufficiently large compact set Ω_1 in $(s_{p1}, \tilde{W}_{p1}, \eta_1)$, for small enough initial values and for small enough disturbance and residual NN error follows $\Delta F_y = 0$. When the saturation does not occur, we know $\eta_1 \rightarrow 0$, thus the conclusions of the closed-loop systems are

the same as in Theorem 1.

Moreover, we use a Lyapunov function as:

$$V_{p1} = \frac{1}{2}s_{p1}^2 + \frac{1}{2}\tilde{W}_{p1}^T \Gamma_{p1}^{-1} \tilde{W}_{p1} + \frac{1}{2}\eta_1^2 \quad (66)$$

The time derivate of \dot{V}_{p1} can be calculated along (20) with (49) as:

$$\begin{aligned} \dot{V}_{p1} &= -k_{p1}s_{p1}^2 + s_{p1}\varepsilon_{p1} + k_o\eta_1 s_{p1} - \sigma\tilde{W}_{p1}^T P_{p1}\tilde{W}_{p1} + \sigma\tilde{W}_{p1}^T \Delta_{p1} \\ &\quad + \eta_1(-k_o\eta_1 + \theta_0\Delta F_y) \\ &\leq -(k_{p1} - \frac{1}{2\eta_{sc1}} - \frac{k_o}{2\eta_{sc1}})s_{p1}^2 - \sigma(\sigma_{p1} - \frac{1}{2\eta_{sc1}})\|\tilde{W}_{p1}\|^2 \\ &\quad - (k_o - \frac{k_o\eta_{sc1}}{2} - \frac{1}{2\eta_{sc1}})\eta_1^2 + \frac{\eta_{sc1}}{2}(\varepsilon_{p1N}^2 + \sigma\varepsilon_{p1Nf}^2 + (\theta_0\Delta F_y)^2) \\ &\leq -\tilde{\mu}_{p1}V_{p1} + \gamma_{p1} \end{aligned} \quad (67)$$

where $\tilde{\mu}_{p1} = \min\{2(k_{p1} - 1/2\eta_{sc1} + k_o/2\eta_{sc1}), 2(\sigma(\sigma_{p1} - 1/2\eta_{sc1})), 2(k_o - k_o\eta_{sc1}/2 - 1/2\eta_{sc1})\}$ and $\gamma_{p1} = \eta_{sc1}(\varepsilon_{p1N}^2 + \sigma\varepsilon_{p1Nf}^2 + (\theta_0\Delta F_y)^2)/2$ are positive constants for appropriately designed parameters k_{p1}, η_{sc1}, k_o such that $k_{p1} > 1/2\eta_{sc1} + k_o/2\eta_{sc1}$, $\eta_{sc1} > 1/2\sigma_{p1}$ and $k_o > 1/(2\eta_{sc1} - \eta_{sc1}^2)$. As shown in [40], $\|\theta_0\Delta F_y\|$ has a maximum in a sufficiently large compact set defined by $\Omega_2 = \{s_{p1}, \tilde{W}_{p1}, \eta_1 \mid V_{p1}(s_{p1}, \tilde{W}_{p1}, \eta_1) \leq \Upsilon\}$ for a positive constant Υ . The continuity of the saturation function permits that this set can be defined larger than Ω_1 , i.e. $\Omega_2 \supset \Omega_1$. Moreover, for small disturbance, γ_{p1} can be made small so that the set of ultimate boundedness is a true subset of Ω_2 , even Ω_1 . Thus, the control error s_{p1} is still bounded so that x_1 is retained within the prescribed boundary. \square

REFERENCE

- [1] D. Hrovat, "Optimal active suspension structures for quarter-car vehicle models," *Automatica*, vol. 26, no. 5, pp. 845-860, 1990.
- [2] D. Cao, X. Song, and M. Ahmadian, "Editors's perspectives: road vehicle suspension design, dynamics, and control," *Veh. Syst. Dyn.*, vol. 49, no. 1-2, pp. 3-28, 2011.
- [3] W. Sun, H. Gao, and O. Kaynak, "Finite Frequency Control for Vehicle Active Suspension Systems," *IEEE Trans. Control Syst. Technol.*, vol. 19, no. 2, pp. 416-422, 2011.
- [4] V. Sankaranarayanan, M. E. Emekli, B. A. Gilvenc, L. Guvenc, E. S. Ozturk, E. S. Ersolmaz, I. E. Eyol, and M. Sinal, "Semiactive suspension control of a light commercial vehicle," *IEEE/ASME Trans. Mechatronics*, vol. 13, no. 5, pp. 598-604, 2008.
- [5] M. Canale, M. Milanese, and C. Novara, "Semi-active suspension control using 'fast' model-predictive techniques," *IEEE Trans. Control Syst. Technol.*, vol. 14, no. 6, pp. 1034-1046, 2006.
- [6] S. M. Savaresi and C. Spelta, "A single-sensor control strategy for semi-active suspensions," *IEEE Trans. Control Syst. Technol.*, vol. 17, no. 1, pp. 143-152, 2009.
- [7] M. Fallah, R. B. Bhat, and W. F. Xie, "Optimized Control of Semiactive Suspension Systems Using H Robust Control Theory and Current Signal Estimation," *IEEE/ASME Trans. Mechatronics*, vol. 17, no. 4, pp. 767-778, 2012.
- [8] H. Chen and K.-H. Guo, "Constrained H^∞ control of active suspensions: an LMI approach," *IEEE Trans. Control Syst. Technol.*, vol. 13, no. 3, pp. 412-421, 2005.

- [9] S. Lee and W.-j. Kim, "Active suspension control with direct-drive tubular linear brushless permanent-magnet motor," *IEEE Trans. Control Syst. Technol.*, vol. 18, no. 4, pp. 859-870, 2010.
- [10] D. Hrovat, "Survey of advanced suspension developments and related optimal control applications," *Automatica*, vol. 33, no. 10, pp. 1781-1817, 1997.
- [11] N. Yagiz and Y. Hacioglu, "Backstepping control of a vehicle with active suspensions," *Control Eng. Pract.*, vol. 16, no. 12, pp. 1457-1467, 2008.
- [12] I. Fialho and G. J. Balas, "Road adaptive active suspension design using linear parameter-varying gain-scheduling," *IEEE Trans. Control Syst. Technol.*, vol. 10, no. 1, pp. 43-54, 2002.
- [13] S.-J. Huang and H.-Y. Chen, "Adaptive sliding controller with self-tuning fuzzy compensation for vehicle suspension control," *Mechatronics*, vol. 16, no. 10, pp. 607-622, 2006.
- [14] G. Koch and T. Kloiber, "Driving State Adaptive Control of an Active Vehicle Suspension System," *IEEE Trans. Control Syst. Technol.*, vol. 22, no. 1, pp. 44-57, 2014.
- [15] L. Zuo, J. J. Slotine, and S. A. Nayfeh, "Model reaching adaptive control for vibration isolation," *IEEE Trans. Control Syst. Technol.*, vol. 13, no. 4, pp. 611-617, 2005.
- [16] V. J. S. Leite and P. L. D. Peres, "Pole location control design of an active suspension system with uncertain parameters," *Veh. Syst. Dyn.*, vol. 43, no. 8, pp. 561-579, 2005.
- [17] H. Du and N. Zhang, "H control of active vehicle suspensions with actuator time delay," *Journal of sound and vibration*, vol. 301, no. 1, pp. 236-252, 2007.
- [18] A. Akbari and B. Lohmann, "Output feedback H/GH₂ preview control of active vehicle suspensions: a comparison study of LQG preview," *Veh. Syst. Dyn.*, vol. 48, no. 12, pp. 1475-1494, 2010.
- [19] E. Kayacan, Y. Oniz, and O. Kaynak, "A grey system modeling approach for sliding-mode control of antilock braking system," *IEEE Trans. Ind. Electron.*, vol. 56, no. 8, pp. 3244-3252, 2009.
- [20] M. Zapateiro, N. Luo, H. R. Karimi, and J. Vehi, "Vibration control of a class of semiactive suspension system using neural network and backstepping techniques," *Mechanical Systems and Signal Processing*, vol. 23, no. 6, pp. 1946-1953, 2009.
- [21] W. Sun, H. Gao, and O. Kaynak, "Adaptive backstepping control for active suspension systems with hard constraints," *IEEE/ASME Trans. Mechatronics*, vol. 18, no. 3, pp. 1072-1079, 2013.
- [22] J.-J. E. Slotine and W. Li, *Applied nonlinear control*, vol. 199. Englewood Cliffs: Prentice-Hall Englewood Cliffs, NJ, 1991.
- [23] C. P. Bechlioulis and G. A. Rovithakis, "Robust adaptive control of feedback linearizable MIMO nonlinear systems with prescribed performance," *IEEE Trans. Autom. Control*, vol. 53, no. 9, pp. 2090-2099, 2008.
- [24] J. Na, "Adaptive prescribed performance control of nonlinear systems with unknown dead zone," *International Journal of Adaptive Control and Signal Processing*, vol. 27, no. 5, pp. 426-446, 2013.
- [25] J. Na, Q. Chen, X. Ren, and Y. Guo, "Adaptive prescribed performance motion control of servo mechanisms with friction compensation," *IEEE Trans. Ind. Electron.*, vol. 61, no. 1, pp. 486-494, 2014.
- [26] W. Meng, Q. Yang, and Y. Sun, "Adaptive neural control of nonlinear MIMO systems with time-varying output constraints," *IEEE Trans. Neural Netw. Learn. Syst.*, vol. 26, no. 5, pp. 1074-1085, 2015.
- [27] J. Na, M. N. Mahyuddin, G. Herrmann, X. Ren, and P. Barber, "Robust adaptive finite - time parameter estimation and control for robotic systems," *International Journal of Robust and Nonlinear Control*, vol. 25, no. 16, pp. 3045-3071, 2015.
- [28] J. Na, M. N. Mahyuddin, G. Herrmann, and X. Ren, "Robust adaptive finite-time parameter estimation for linearly parameterized nonlinear systems," In: *Proceeding of 2013 32nd Chinese, Control Conference (CCC)*, pp. 1735-1741, 2013.
- [29] C. P. Bechlioulis and G. A. Rovithakis, "Adaptive control with guaranteed transient and steady state tracking error bounds for strict feedback systems," *Automatica*, vol. 45, no. 2, pp. 532-538, 2009.
- [30] S.-I. Han and J.-M. Lee, "Recurrent fuzzy neural network backstepping control for the prescribed output tracking performance of nonlinear dynamic systems," *ISA Trans.*, vol. 53, no. 1, pp. 33-43, 2014.
- [31] X. Ren, F. L. Lewis, and J. Zhang, "Neural network compensation control for mechanical systems with disturbances," *Automatica*, vol. 45, no. 5, pp. 1221-1226, 2009.
- [32] J. Na, X. Ren, G. Herrmann, and Z. Qiao, "Adaptive neural dynamic surface control for servo systems with unknown dead-zone," *Control Eng. Pract.*, vol. 19, no. 11, pp. 1328-1343, 2011.
- [33] J. Na, X. Ren, and D. Zheng, "Adaptive control for nonlinear pure-feedback systems with high-order sliding mode observer," *IEEE Trans. Neural Netw. Learn. Syst.*, vol. 24, no. 3, pp. 370-382, 2013.
- [34] B. Xu, C. Yang, and Z. Shi, "Reinforcement learning output feedback NN control using deterministic learning technique," *IEEE Trans. Neural Netw. Learn. Syst.*, vol. 25, no. 3, pp. 635-641, 2014.
- [35] Y.-J. Liu, L. Tang, S. Tong, C. P. Chen, and D.-J. Li, "Reinforcement learning design-based adaptive tracking control with less learning parameters for nonlinear discrete-time MIMO systems," *IEEE Trans. Neural Netw. Learn. Syst.*, vol. 26, no. 1, pp. 165-176, 2015.
- [36] H. Imine and T. Madani, "Heavy vehicle suspension parameters identification and estimation of vertical forces: experimental results," *International Journal of Control*, vol. 88, no. 2, pp. 324-334, 2015.
- [37] M. N. Mahyuddin, J. Na, G. Herrmann, X. Ren, and P. Barber, "Adaptive observer-based parameter estimation with application to road gradient and vehicle mass estimation," *IEEE Trans. Ind. Electron.*, vol. 61, no. 6, pp. 2851-2863, 2014.
- [38] Y. Huang, J. Na, X. Wu, X. Liu, and Y. Guo, "Adaptive control of nonlinear uncertain active suspension systems with prescribed performance," *ISA Trans.*, vol. 54, pp. 145-155, 2015.
- [39] S. S. Ge, C. C. Hang, T. H. Lee, and T. Zhang, *Stable adaptive neural network control*, vol. 13: Springer Science & Business Media, 2013.
- [40] W. Sun, Z. Zhao, and H. Gao, "Saturated adaptive robust control for active suspension systems," *IEEE Trans. Ind. Electron.*, vol. 60, no. 9, pp. 3889-3896, 2013.
- [41] M. C. Turner and I. Postlethwaite, "A new perspective on static and low order anti-windup synthesis," *International Journal of Control*, vol. 77, no. 1, pp. 27-44, 2004.
- [42] G. Herrmann, M. C. Turner, and I. Postlethwaite, "Discrete-time and sampled-data anti-windup synthesis: stability and performance," *International Journal of Systems Science*, vol. 37, no. 2, pp. 91-113, 2006.
- [43] S. Savaresi, C. Poussot-Vassal, C. Spelta, O. Sename, L. Dugard, *Semi-Active Suspension Control Design for Vehicles*, Elsevier, 2010.